Marine Structures 22 (2009) 387–437

Contents lists available at ScienceDirect

Marine Structures

journal homepage: www.elsevier.com/locate/marstruc

An advanced theory of thin-walled girders with application to ship vibrations

I. Senjanović*, S. Tomašević, N. Vladimir

University of Zagreb, Faculty of Mechanical Engineering and Naval Architecture, I. Lučića 5, 10000 Zagreb, Croatia

ARTICLE INFO

Article history:
Received 8 July 2008
Received in revised form 7 January 2009
Accepted 24 March 2009

Keywords:
Thin-walled girder theory
Beam model
Coupled vibrations
Container ship
FEM

ABSTRACT

The paper presents an outline of the advanced theory of thin-walled girders. The improvement includes shear influence on torsion as an extension of shear influence on bending. The analogy between bending and torsion is recognized and pointed out throughout the paper. Complete differential equations of coupled flexural and torsional vibrations for a prismatic girder are derived. In addition, the 8 d.o.f. beam finite element, utilizing the energy approach, is constituted with stiffness and mass matrices, and load vectors. The paper describes determining of geometrical properties of multi-cell open cross-sections by employing the strip element method. Numerical procedures for vibration analyses are outlined. Furthermore, dry natural vibrations of a VLCS (Very Large Container Ship) are analysed by 1D FEM model as a prerogative for hydroelastic analyses of these relatively flexible vessels. Influence of transverse bulkheads is taken into account by increasing torsional stiffness of the ship hull proportionally to their deformation energies. Validation of 1D FEM model is checked by correlation analysis with the vibration response of the fine 3D FEM model.

* Corresponding author. Tel.: +385 16168142; fax: +385 16156940.
E-mail address: ivo.senjanovic@fsb.hr (I. Senjanović).

0951-8339/$ – see front matter © 2009 Elsevier Ltd. All rights reserved.
doi:10.1016/j.marstruc.2009.03.004

Nomenclature

A	cross-section area
A_i	integration constants
A_s	shear area
a_k, b_k, c_k, d_k, e_k, f_k,	coefficients of shape functions
B_w	warping bimoment
b	one half of bulkhead breadth
C	energy coefficient
c	eccentricity
E	Young's modulus
E_{tot}	total energy
f	normal stress flow
G	shear modulus
g	shear stress flow
H	ship height
I_b	moment of inertia of cross-section
I_s	shear inertia modulus
I_t	torsional modulus
I_w	warping modulus
i, j, k	indexes
J_b	moment of inertia of distributed mass
J_t^0 ,J_t	polar moment of inertia of distributed mass about centre of gravity and shear centre
J_w	bimoment of inertia of distributed mass about warping centre
L, l	length
M	bending moment
m	distributed mass
n	mode number
Q	shear force
q	distributed load
T	torque
T_t	torsional torque
T_w	warping torque
t	time
U	strain energy
w	deflection
w_b	bending deflection
w_s	shear deflection
u, v	membrane displacements
x, y, z	coordinates
z_C, z_S, z_G	coordinate of centroid, shear centre and gravity centre
$[C]$	damping matrix
$[D]$	elasticity matrix
$[K]$, $[k]$	stiffness matrices
$[L]$	deformation matrix
$[M]$, $[m]$	mass matrices
$[T]$	transformation matrix
$\{F\}$, $\{f\}$	force vectors

$\{P\}$, $\{R\}$	force vectors
$\{U\}$, $\{V\}$	displacement vectors
$\{\Delta\}$, $\{\delta\}$	displacement vectors
α, η	vibration coefficients
β, γ	stiffness ratios
ζ	damping coefficient
ϑ	variation of twist angle
μ	distributed torque
ν	Poisson's coefficient
ξ	non-dimensional coordinate
σ	normal stress
τ	shear stress
φ	rotation angle
ψ	twist angle
ψ_t	pure twist angle
ψ_s	shear twist angle
ω	natural frequency
$[\phi]$	matrix of shape functions

1. Introduction

Increased sea transport requires building of ultra large container ships which are quite flexible [1]. Therefore, their strength has to be checked by hydroelastic analysis [2]. The methodology of hydroelastic analysis is described in [3]. It includes the definition of the structural model, ship and cargo mass distributions, and geometrical model of ship wetted surface. Hydroelastic analysis is based on the modal superposition method. First, dry natural vibrations of ship hull are calculated. Then, modal hydrostatic stiffness, modal added mass, modal damping and modal wave load are determined. Finally, the calculation of wet natural vibrations is performed and transfer functions for determining ship structural response to wave excitation are obtained [4,5]. The approach is checked by the model test of the flexible barge [6,7].

The intention of this paper is to present an advanced numerical procedure based on the beam and thin-walled girder theories for reliable calculation of dry natural vibrations of container ships, as an important step in their hydroelastic analysis. A ship hull, as an elastic nonprismatic thin-walled girder, performs longitudinal, vertical, horizontal and torsional vibrations. Since the cross-sectional centre of gravity and centroid, as well as the shear centre positions are not identical, coupled longitudinal and vertical, and horizontal and torsional vibrations occur, respectively.

The distance between the centre of gravity and centroid for longitudinal and vertical vibrations, as well as distance between the former and shear centre for horizontal and torsional vibrations are negligible for conventional ships. Therefore, in the above cases ship hull vibrations are usually analysed separately. However, the shear centre in ships with large hatch openings is located outside the cross-section, i.e. below the keel, and therefore the coupling of horizontal and torsional vibrations is extremely high.

The above problem is rather complicated due to geometrical discontinuity of the hull cross-section. The accuracy of the solution depends on the reliability of stiffness parameters determination, i.e. of bending, shear, torsional and warping moduli. The finite element method is a powerful tool to solve the above problem in a successful way.

One of the first solutions for coupled horizontal and torsional hull vibrations, dealing with the finite element technique, is given in [8,9]. Generalised and improved solutions are presented in [10,11]. In all these references, the determination of hull stiffness is based on the classical thin-walled girder theory, which does not give a satisfactory value for the warping modulus of the open cross-section [12,13].

Apart from that, the fixed values of stiffness moduli are determined, so that the application of the beam theory for hull vibration analysis is limited to a few lowest natural modes only. Otherwise, if the mode dependent stiffness parameters are used the application of the beam theory can be extended up to the tenth natural mode [14–16].

Based on the above described state-of-the-art and inspired motivation, this paper brings some novelties and improvements to the thin-walled girder theory. Shear influence on torsion, as an extension of its influence on bending, is taken into account. Analogy between bending and torsion is used as a sign-post. All the relevant stiffness and mass parameters are included in the differential equations of coupled flexural and torsional vibrations. A more complete beam finite element with eight degrees of freedom is developed. The application of the advanced theory is illustrated in the case of a very large container vessel. The influence of transverse bulkheads is incorporated in the hull stiffness [17,18]. The validity of the improved theory is checked by correlation of the 1D FEM vibration response with that obtained by 3D FEM analysis.

2. Differential equations of beam vibrations

Referring to the flexural beam theory [19,20], the total beam deflection, w, consists of the bending deflection, w_b, and the shear deflection, w_s, while the angle of cross-section rotation depends only on the former, Fig. 1

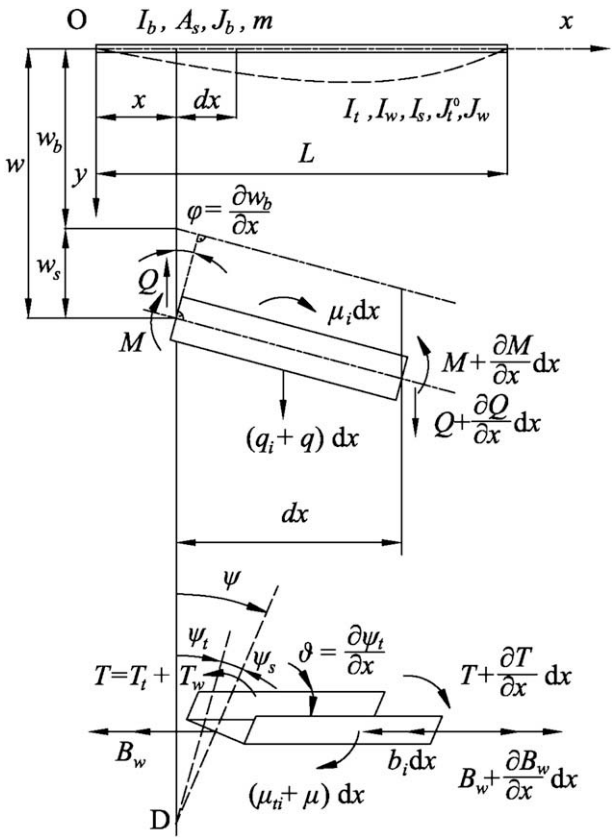

Fig. 1. Beam bending and torsion.

$$w = w_b + w_s, \quad \varphi = \frac{\partial w_b}{\partial x}. \tag{1}$$

The cross-sectional forces are the bending moment and the shear force

$$M = -EI_b \frac{\partial \varphi}{\partial x}, \tag{2}$$

$$Q = GA_s \frac{\partial w_s}{\partial x}, \tag{3}$$

where E and G are Young's and shear modulus, respectively, while I_b and A_s are the moment of inertia of cross-section and shear area, respectively.

The inertia load consists of the distributed transverse load, q_i, and the bending moment, μ_i, and in the case of coupled horizontal and torsional vibration is specified as

$$q_i = -m\left(\frac{\partial^2 w}{\partial t^2} + c\frac{\partial^2 \psi}{\partial t^2}\right), \tag{4}$$

$$\mu_i = -J_b \frac{\partial^2 \varphi}{\partial t^2}, \tag{5}$$

where m is the distributed ship and added mass, J_b is the moment of inertia of ship mass about z-axis, and c is the distance between the centre of gravity and the shear centre, $c = z_G - z_S$, Fig. 2.

Concerning torsion, the total twist angle, ψ, consists of the pure twist angle, ψ_t, and the shear contribution, ψ_s, while the second beam displacement, which causes warping of cross-section, is variation of the pure twist angle, i.e. Fig. 1 [18]

$$\psi = \psi_t + \psi_s, \quad \vartheta = \frac{\partial \psi_t}{\partial x}. \tag{6}$$

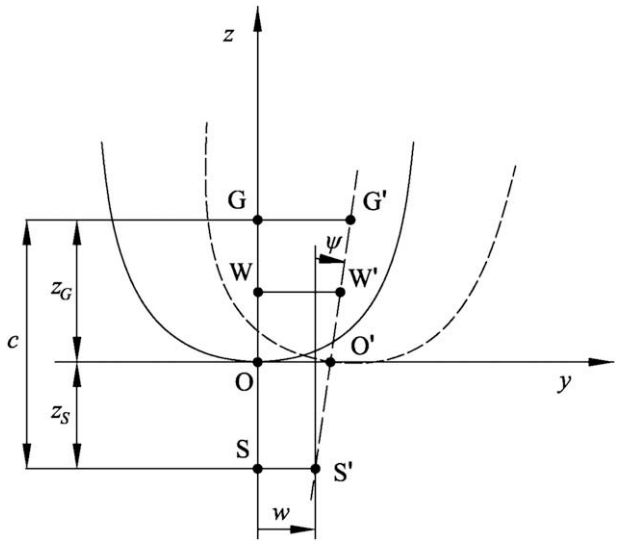

Fig. 2. Cross-section of a thin-walled girder.

The cross-sectional forces include the pure torsional torque, T_t, warping bimoment, B_w, and additional torque due to restrained warping, T_w

$$T_t = GI_t\vartheta, \tag{7}$$

$$B_w = -EI_w\frac{\partial\vartheta}{\partial x}, \tag{8}$$

$$T_w = GI_s\frac{\partial\psi_s}{\partial x}, \tag{9}$$

where I_t, I_w and I_s are the torsional modulus, warping modulus and shear inertia modulus, respectively.

The inertia load consists of the distributed torque, μ_{ti}, and the bimoment, b_i, presented in the following form:

$$\mu_{ti} = -J_t\frac{\partial^2\psi}{\partial t^2} - mc\frac{\partial^2 w}{\partial t^2}, \tag{10}$$

$$b_i = -J_w\frac{\partial^2\vartheta}{\partial t^2}, \tag{11}$$

where J_t is the polar moment of inertia of ship and added mass about the shear centre, and J_w is the bimoment of inertia of ship mass about the warping centre, Fig. 2.

Considering the equilibrium of a differential element, one can write for flexural vibrations

$$\frac{\partial M}{\partial x} = Q + \mu_i, \tag{12}$$

$$\frac{\partial Q}{\partial x} = -q_i - q, \tag{13}$$

and for torsional vibrations [17]

$$\frac{\partial B_w}{\partial x} = T_w + b_i, \tag{14}$$

$$\frac{\partial T_t}{\partial x} + \frac{\partial T_w}{\partial x} = -\mu_{ti} - \mu. \tag{15}$$

The above equations can be reduced to two coupled partial differential equations as follows. Substituting Eqs. (2) and (3) into (12) yields

$$\frac{\partial w_s}{\partial x} = -\frac{EI_b}{GA_s}\frac{\partial^2\varphi}{\partial x^2} + \frac{J_b}{GA_s}\frac{\partial^2\varphi}{\partial t^2}. \tag{16}$$

By inserting Eqs. (3) and (4) into (13) leads to

$$EI_b\frac{\partial^4\varphi}{\partial x^4} + m\frac{\partial^2\varphi}{\partial t^2} - \left(J_b + m\frac{EI_b}{GA_s}\right)\frac{\partial^4\varphi}{\partial x^2\partial t^2} + \frac{mJ_b}{GA_s}\frac{\partial^4\varphi}{\partial t^4} + mc\frac{\partial^3\psi}{\partial x\partial t^2} = \frac{\partial q}{\partial x}. \tag{17}$$

In similar way, substituting Eqs. (8) and (9) into (14) yields

$$\frac{\partial \psi_s}{\partial x} = -\frac{EI_w}{GI_s}\frac{\partial^2 \vartheta}{\partial x^2} + \frac{J_w}{GI_s}\frac{\partial^2 \vartheta}{\partial t^2}. \tag{18}$$

By inserting Eqs. (7), (9) and (10) into (15) one finds

$$EI_w\frac{\partial^4 \vartheta}{\partial x^4} - GI_t\frac{\partial^2 \vartheta}{\partial x^2} + J_t\frac{\partial^2 \vartheta}{\partial t^2} - \left(J_w + J_t\frac{EI_w}{GI_s}\right)\frac{\partial^4 \vartheta}{\partial x^2 \partial t^2} + \frac{J_w}{GI_s}\frac{\partial^4 \vartheta}{\partial t^4} + mc\frac{\partial^3 w}{\partial x \partial t^2} = \frac{\partial \mu}{\partial x}. \tag{19}$$

Furthermore, ψ in (17) can be split into $\psi_t + \psi_s$ and the later term can be expressed with (18). Similar substitution can be done for $w = w_b + w_s$ in (19), where w_s is given with (16). Thus, taking into account that $\varphi = \partial w_b/\partial x$ and $\vartheta = \partial \psi_t/\partial x$, Eqs. (17) and (19) after integration per x read

$$EI_b\frac{\partial^4 w_b}{\partial x^4} + m\frac{\partial^2 w_b}{\partial t^2} - \left(J_b + m\frac{EI_b}{GA_s}\right)\frac{\partial^4 w_b}{\partial x^2 \partial t^2} + \frac{mJ_b}{GA_s}\frac{\partial^4 w_b}{\partial t^4} + mc\left(\frac{\partial^2 \psi_t}{\partial t^2} - \frac{EI_w}{GI_s}\frac{\partial^4 \psi_t}{\partial x^2 \partial t^2} + \frac{J_w}{GI_s}\frac{\partial^4 \psi_t}{\partial t^4}\right) = q \tag{20}$$

$$EI_w\frac{\partial^4 \psi_t}{\partial x^4} - GI_t\frac{\partial^2 \psi_t}{\partial x^2} + J_t\frac{\partial^2 \psi_t}{\partial t^2} - \left(J_w + J_t\frac{EI_w}{GI_s}\right)\frac{\partial^4 \psi_t}{\partial x^2 \partial t^2} + \frac{J_w}{GI_s}\frac{\partial^4 \psi_t}{\partial t^4} + mc\left(\frac{\partial^2 w_b}{\partial t^2} - \frac{EI_b}{GA_s}\frac{\partial^4 w_b}{\partial x^2 \partial t^2} + \frac{J_b}{GA_s}\frac{\partial^4 w_b}{\partial t^4}\right) = \mu. \tag{21}$$

After solving Eqs. (20) and (21) the total deflection and twist angle are obtained by employing (16) and (18)

$$w = w_b + w_s = w_b - \frac{EI_b}{GA_s}\frac{\partial^2 w_b}{\partial x^2} + \frac{J_b}{GA_s}\frac{\partial^2 w_b}{\partial t^2} + f(t), \tag{22}$$

$$\psi = \psi_t + \psi_s = \psi_t - \frac{EI_w}{GI_s}\frac{\partial^2 \psi_t}{\partial x^2} + \frac{J_w}{GI_s}\frac{\partial^2 \psi_t}{\partial t^2} + g(t), \tag{23}$$

where $f(t)$ and $g(t)$ are integration functions, which depend on initial conditions.

The main purpose of developing differential equations of vibrations (20) and (21) is to get insight into their constitution, position and role of the stiffness and mass parameters, and coupling, which is realized through the inertia terms. If the pure torque T_t is excluded from the above theoretical consideration, it is obvious that the complete analogy between bending and torsion exists, [17].

Application of Eqs. (20) and (21) is limited to prismatic girders. It is illustrated in case of uncoupled torsional natural vibrations of a uniform beam in Appendix A. For more complex problems, like ship hull, the finite element method, as a powerful tool, is on disposal.

The shape functions of beam finite element for vibration analysis have to satisfy the following consistency relations for harmonic vibrations obtained from Eqs. (22) and (23), [20]

$$w = w_b + w_s = \left(1 - \omega^2\frac{J_b}{GA_s}\right)w_b - \frac{EI_b}{GA_s}\frac{\mathrm{d}^2 w_b}{\mathrm{d}x^2}, \tag{24}$$

$$\psi = \psi_t + \psi_s = \left(1 - \omega^2\frac{J_w}{GI_s}\right)\psi_t - \frac{EI_w}{GI_s}\frac{\mathrm{d}^2 \psi_t}{\mathrm{d}x^2}. \tag{25}$$

3. Beam finite element

The properties of a finite element for the coupled horizontal and torsional vibration analysis can be derived from the total element energy. The total energy consists of the strain energy, the kinetic energy, the work of the external lateral load, q, and the torque, μ, and the work of the boundary forces. Thus, according to [9,20],

$$\begin{aligned} E_{tot} = & \frac{1}{2}\int_0^l \left[EI_b\left(\frac{\partial^2 w_b}{\partial x^2}\right)^2 + GA_s\left(\frac{\partial w_s}{\partial x}\right)^2 + EI_w\left(\frac{\partial^2 \psi_t}{\partial x^2}\right)^2 + GI_s\left(\frac{\partial \psi_s}{\partial x}\right)^2 + GI_t\left(\frac{\partial \psi_t}{\partial x}\right)^2 \right] \mathrm{d}x \\ & + \frac{1}{2}\int_0^l \left[m\left(\frac{\partial w}{\partial t}\right)^2 + J_b\left(\frac{\partial^2 w_b}{\partial x \partial t}\right)^2 + 2mc\frac{\partial w}{\partial t}\frac{\partial \psi}{\partial t} + J_w\left(\frac{\partial^2 \psi_t}{\partial x \partial t}\right)^2 + J_t\left(\frac{\partial \psi}{\partial t}\right)^2 \right] \mathrm{d}x \\ & - \int_0^l (qw + \mu\psi)\mathrm{d}x + (Qw - M\varphi + T\psi + B_w\vartheta)_0^l, \end{aligned} \tag{26}$$

where l is the element length.

Since the beam has four displacements, $w, \varphi, \psi, \vartheta$, a two-node finite element has eight degrees of freedom, i.e. four nodal shear-bending and torsion-warping displacements respectively, Fig. 3,

$$\{U\} = \begin{Bmatrix} w(0) \\ \varphi(0) \\ w(l) \\ \varphi(l) \end{Bmatrix}, \quad \{V\} = \begin{Bmatrix} \psi(0) \\ \vartheta(0) \\ \psi(l) \\ \vartheta(l) \end{Bmatrix}. \tag{27}$$

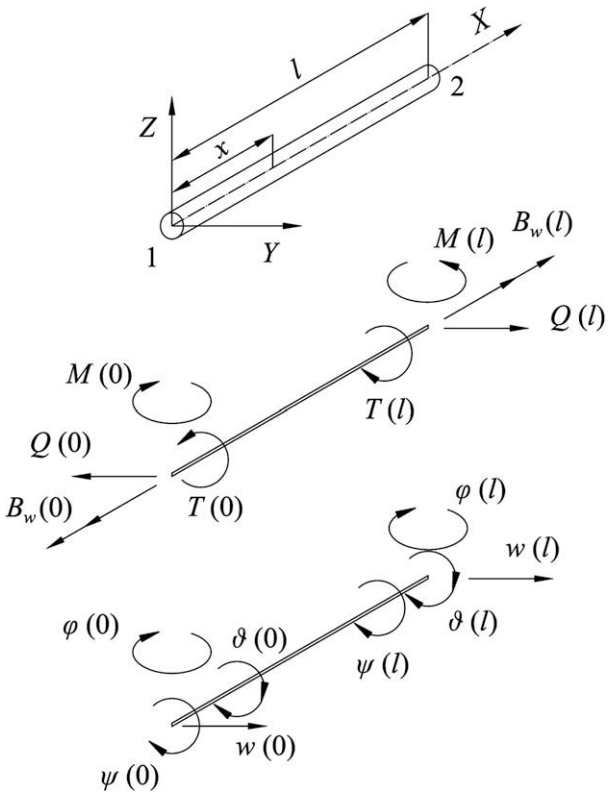

Fig. 3. Beam finite element.

Therefore, the basic beam displacements, w_b and ψ_t, can be presented as the third-order polynomials

$$\begin{aligned} w_b &= \langle a_k \rangle \left\{ \xi^k \right\}, \quad \psi_t = \langle d_k \rangle \left\{ \xi^k \right\}, \ k = 0,1,2,3, \\ \xi &= \frac{x}{l}, \ \langle \ldots \rangle = \{\ldots\}^T. \end{aligned} \tag{28}$$

Furthermore, satisfying alternately the unit value for one of the nodal displacement $\{U\}$ and zero values for the remaining displacements, and doing the same for $\{V\}$, it follows that:

$$\begin{aligned} w_b &= \langle w_{bi} \rangle \{U\}, \ w_s = \langle w_{si} \rangle \{U\}, \ w = \langle w_i \rangle \{U\}, \\ \psi_t &= \langle \psi_{ti} \rangle \{V\}, \ \psi_s = \langle \psi_{si} \rangle \{V\}, \ \psi = \langle \psi_i \rangle \{V\}, \ i = 1,2,3,4, \end{aligned} \tag{29}$$

where w_{bi}, w_{si}, w_i and ψ_{ti}, ψ_{si}, ψ_i are the shape functions specified below by employing relations (24) and (25)

$$\begin{aligned} w_{bi} &= \langle a_{ik} \rangle \left\{ \xi^k \right\}, \ w_{si} = \langle b_{ik} \rangle \left\{ \xi^k \right\}, \ w_i = \langle c_{ik} \rangle \left\{ \xi^k \right\} \\ \psi_{ti} &= \langle d_{ik} \rangle \left\{ \xi^k \right\}, \ \psi_{si} = \langle e_{ik} \rangle \left\{ \xi^k \right\}, \ \psi_i = \langle f_{ik} \rangle \left\{ \xi^k \right\} \end{aligned} \tag{30}$$

$$[a_{ik}] = \frac{1}{\alpha(\alpha+12\beta)} \begin{bmatrix} \alpha+6\beta & 0 & -3\alpha & 2\alpha \\ -4\beta(\alpha+3\beta)l & \alpha(\alpha+12\beta)l & -2\alpha(\alpha+3\beta)l & \alpha^2 l \\ 6\beta & 0 & 3\alpha & -2\alpha \\ -2\beta(\alpha-6\beta)l & 0 & -\alpha(\alpha-6\beta)l & \alpha^2 l \end{bmatrix} \tag{31}$$

$$\begin{aligned} b_{i0} &= -(1-\alpha)a_{i0} - 2\beta a_{i2} \\ b_{i1} &= -(1-\alpha)a_{i1} - 6\beta a_{i3} \\ b_{i2} &= -(1-\alpha)a_{i2} \\ b_{i3} &= -(1-\alpha)a_{i3}, \end{aligned} \tag{32}$$

$$[c_{ik}] = [a_{ik}] + [b_{ik}], \quad i = 1,2,3,4, \ k = 0,1,2,3 \tag{33}$$

$$\alpha = 1 - \omega^2 \frac{J_b}{GA_s}, \quad \beta = \frac{EI_b}{GA_s l^2} \tag{34}$$

Constitution of torsional matrices $[d_{ik}]$, $[e_{ik}]$ and $[f_{ik}]$ is the same as $[a_{ik}]$, $[b_{ik}]$ and $[c_{ik}]$, but parameters α and β have to be exchanged with

$$\eta = 1 - \omega^2 \frac{J_w}{GI_s}, \quad \gamma = \frac{EI_w}{GI_s l^2} \tag{35}$$

according to (25).

By substituting Eqs. (29) into (26) one obtains

$$\begin{aligned} E_{tot} = {} & \frac{1}{2} \begin{Bmatrix} U \\ V \end{Bmatrix}^T \begin{bmatrix} k_{bs} & 0 \\ 0 & k_{ws}+k_t \end{bmatrix} \begin{Bmatrix} U \\ V \end{Bmatrix} + \frac{1}{2} \begin{Bmatrix} \dot{U} \\ \dot{V} \end{Bmatrix}^T \begin{bmatrix} m_{sb} & m_{st} \\ m_{ts} & m_{tw} \end{bmatrix} \begin{Bmatrix} \dot{U} \\ \dot{V} \end{Bmatrix} - \begin{Bmatrix} q \\ \mu \end{Bmatrix}^T \begin{Bmatrix} U \\ V \end{Bmatrix} \\ & - \begin{Bmatrix} P \\ R \end{Bmatrix}^T \begin{Bmatrix} U \\ V \end{Bmatrix}, \end{aligned} \tag{36}$$

where, assuming constant values of the element properties,

$[k]_{bs} = [EI_b \int_0^l (\mathrm{d}^2 w_{bi}/\mathrm{d}x^2)(\mathrm{d}^2 w_{bj}/\mathrm{d}x^2)\mathrm{d}x + GA_s \int_0^l (\mathrm{d}w_{si}/\mathrm{d}x)(\mathrm{d}w_{sj}/\mathrm{d}x)\mathrm{d}x]$ – *bending-shear stiffness matrix*,

$[k]_{ws} = [EI_w \int_0^l (\mathrm{d}^2\psi_{ti}/\mathrm{d}x^2)(\mathrm{d}^2\psi_{tj}/\mathrm{d}x^2)\mathrm{d}x + GI_s \int_0^l (\mathrm{d}\psi_{si}/\mathrm{d}x)(\mathrm{d}\psi_{sj}/\mathrm{d}x)\mathrm{d}x]$ – *warping-shear stiffness matrix*,

$[k]_t = [GI_t \int_0^l (\mathrm{d}\psi_{ti}/\mathrm{d}x)(\mathrm{d}\psi_{tj}/\mathrm{d}x)\mathrm{d}x]$ – *torsion stiffness matrix*,

$[m]_{sb} = [m \int_0^l w_i w_j \mathrm{d}x + J_b \int_0^l (\mathrm{d}w_{bi}/\mathrm{d}x)(\mathrm{d}w_{bj}/\mathrm{d}x)\mathrm{d}x]$ – *shear-bending mass matrix*,

$[m]_{tw} = [J_t \int_0^l \psi_i \psi_j \mathrm{d}x + J_w \int_0^l (\mathrm{d}\psi_{ti}/\mathrm{d}x)(\mathrm{d}\psi_{tj}/\mathrm{d}x)\mathrm{d}x]$ – *torsion-warping mass matrix*,

$[m]_{st} = [mc \int_0^l w_i \psi_j \mathrm{d}x\Big], \quad [m]_{ts} = [m]_{st}^{\mathrm{T}}$ – *shear-torsion mass matrix*,

$$\begin{aligned} \{q\} &= \left\{ \int_0^l q w_j \mathrm{d}x \right\} \quad - \quad \textit{shear load vector}, \\ \{\mu\} &= \left\{ \int_0^l \mu \psi_j \mathrm{d}x \right\} \quad - \quad \textit{torsion load vector}, \\ i,j &= 1,2,3,4. \end{aligned} \tag{37}$$

The vectors $\{P\}$ and $\{R\}$ represent the shear-bending and torsion-warping nodal forces, respectively,

$$\{P\} = \begin{Bmatrix} -Q(0) \\ M(0) \\ Q(l) \\ -M(l) \end{Bmatrix}, \quad \{R\} = \begin{Bmatrix} -T(0) \\ B_w(0) \\ T(l) \\ -B_w(l) \end{Bmatrix}. \tag{38}$$

The above matrices are specified in Appendix B, as well as the load vectors for linearly distributed loads along the element, i.e.

$$q = q_0 + q_1\xi, \quad \mu = \mu_0 + \mu_1\xi. \tag{39}$$

Also, shape functions of sectional forces are listed in Appendix C.

The total element energy has to be at its minimum. Satisfying the relevant conditions

$$\frac{\partial E_{tot}}{\partial\{U\}} = \{0\}, \quad \frac{\partial E_{tot}}{\partial\{V\}} = \{0\} \tag{40}$$

and employing Lagrange equations of motion, the finite element equation yields

$$\{f\} = [k]\{\delta\} + [m]\left\{\ddot{\delta}\right\} - \{f\}_{q\mu}, \tag{41}$$

where

$$\begin{aligned} &\{f\} = \begin{Bmatrix} P \\ R \end{Bmatrix}, \quad \{f\}_{q\mu} = \begin{Bmatrix} q \\ \mu \end{Bmatrix}, \quad \{\delta\} = \begin{Bmatrix} U \\ V \end{Bmatrix} \\ &[k] = \begin{bmatrix} k_{bs} & 0 \\ 0 & k_{ws} + k_t \end{bmatrix}, \quad [m] = \begin{bmatrix} m_{sb} & m_{st} \\ m_{ts} & m_{tw} \end{bmatrix}. \end{aligned} \tag{42}$$

It is obvious that coupling between the bending and torsion occurs through the mass matrix only, i.e. by the coupling matrices $[m]_{st}$ and $[m]_{ts}$.

4. Finite element transformation

In the finite element equation (41), first the element properties related to bending and then those related to torsion appear. To make an ordinary finite element assembling possible, it is necessary to transform Eq. (41) in such a way that first all properties related to the first node are specified and

then those belonging to the second one. Thus, the rearranged nodal force and displacement vectors read

$$\left\{\tilde{f}\right\} = \begin{Bmatrix} -Q(0) \\ M(0) \\ -T(0) \\ B_w(0) \\ Q(l) \\ -M(l) \\ T(l) \\ -B_w(l) \end{Bmatrix}, \quad \left\{\tilde{\delta}\right\} = \begin{Bmatrix} w(0) \\ \varphi(0) \\ \psi(0) \\ \varphi(0) \\ w(l) \\ \varphi(l) \\ \psi(l) \\ \varphi(l) \end{Bmatrix}. \tag{43}$$

The same transformation has to be done for the load vector $\{f\}_{q\mu}$ resulting in $\{\tilde{f}\}_{q\mu}$. The above vector transformation implies the row and column exchange in the matrices according to the following set form:

	1	2	5	6	3	4	7	8
1	11	12	15	16	13	14	17	18
2	21	22	25	26	23	24	27	28
5	51	52	55	56	53	54	57	58
6	61	62	65	66	63	64	67	68
3	31	32	35	36	33	34	37	38
4	41	42	45	46	43	44	47	48
7	71	72	75	76	73	74	77	78
8	81	82	85	86	83	84	87	88

(44)

The element deflection refers to the shear centre as the origin of a local coordinate system. Since the vertical position of the shear centre varies along the ship's hull, it is necessary to prescribe the element deflection for a common line, in order to be able to assemble the elements. Thus, choosing the x-axis (base line) of the global coordinate system as the referent line, the following relation between the former and the latter nodal deflections exists:

$$\begin{aligned} w(0) &= \overline{w}(0) + z_S\psi(0) \\ w(l) &= \overline{w}(l) + z_S\psi(l), \end{aligned} \tag{45}$$

where z_S is the coordinate of the shear centre, Fig. 2. Other displacements are the same in both coordinate systems. Twist angle ψ does not have influence on the cross-section rotation angle φ. The local displacement vector can be expressed as

$$\left\{\tilde{\delta}\right\} = \left[\tilde{T}\right]\left\{\bar{\tilde{\delta}}\right\}, \tag{46}$$

where $[\tilde{T}]$ is the transformation matrix

$$\left[\tilde{T}\right] = \begin{bmatrix} [T] & [0] \\ [0] & [T] \end{bmatrix}, \quad [T] = \begin{bmatrix} 1 & 0 & z_S & 0 \\ 0 & 1 & 0 & 0 \\ 0 & 0 & 1 & 0 \\ 0 & 0 & 0 & 1 \end{bmatrix}. \tag{47}$$

Since the total element energy is not changed by the above transformations, a new element equation can be derived taking (46) into account. Thus, one obtains in the global coordinate system

$$\left\{\bar{\tilde{f}}\right\} = \left[\bar{\tilde{k}}\right]\left\{\bar{\tilde{\delta}}\right\} + \left[\bar{\tilde{m}}\right]\left\{\ddot{\bar{\tilde{\delta}}}\right\} - \left\{\bar{\tilde{f}}\right\}_{q\mu}, \tag{48}$$

where

$$\left\{\bar{\tilde{f}}\right\} = \left[\tilde{T}\right]^T \left\{\tilde{f}\right\} \qquad \left[\bar{\tilde{k}}\right] = \left[\tilde{T}\right]^T \left[\tilde{k}\right]\left[\tilde{T}\right] \qquad \left[\bar{\tilde{m}}\right] = \left[\tilde{T}\right]^T \left[\tilde{m}\right]\left[\tilde{T}\right] \qquad \left\{\bar{\tilde{f}}\right\}_{q\mu} = \left[\tilde{T}\right]^T \left\{\tilde{f}\right\}_{q\mu}. \tag{49}$$

The first of the above expressions transforms the nodal torques into the form

$$\begin{aligned} -\overline{T}(0) &= -T(0) - z_S Q(0) \\ \overline{T}(l) &= T(l) + z_S Q(l). \end{aligned} \tag{50}$$

5. Numerical procedure for vibration analysis

A ship's hull is modelled by a set of beam finite elements. Their assemblage in the global coordinate system, performed in the standard way, results in the matrix equation of motion, which may be extended by the damping forces

$$[K]\{\Delta\} + [C]\left\{\dot{\Delta}\right\} + [M]\left\{\ddot{\Delta}\right\} = \{F(t)\}, \tag{51}$$

where $[K]$, $[C]$ and $[M]$ are the stiffness, damping and mass matrices, respectively; $\{\Delta\}, \left\{\dot{\Delta}\right\}$ and $\{\ddot{\Delta}\}$ are the displacement, velocity and acceleration vectors, respectively; and $\{F(t)\}$ is the load vector.

In case of natural vibration $\{F(t)\} = \{0\}$ and the influence of damping is rather low for ship structures, so that the damping forces may be ignored. Assuming

$$\{\Delta\} = \{\phi\}e^{i\omega t}, \tag{52}$$

where $\{\phi\}$ and ω are the mode vector and natural frequency respectively, Eq. (51) leads to the eigenvalue problem

$$\left([K] - \omega^2[M]\right)\{\phi\} = \{0\}, \tag{53}$$

which may be solved by employing different numerical methods [21]. The basic one is the determinant search method in which ω is found from the condition

$$\left|[K] - \omega^2[M]\right| = 0 \tag{54}$$

by an iteration procedure. Afterwards, $\{\phi\}$ follows from (53) assuming unit value for one element in $\{\phi\}$.

The forced vibration analysis may be performed by direct integration of Eq. (51), as well as by the modal superposition method. In the latter case the displacement vector is presented in the form

$$\{\Delta\} = [\phi]\{X\}, \tag{55}$$

where $[\phi] = [\{\phi\}]$ is the undamped mode matrix and $\{X\}$ is the generalised displacement vector. Substituting (55) into (51), the modal equation yields

$$[k]\{X\} + [c]\{\dot{X}\} + [m]\left\{\ddot{X}\right\} = \{f(t)\}, \tag{56}$$

where

$$\begin{aligned} [k] &= [\phi]^T[K][\phi] \quad - \quad \textit{modal stiffness matrix} \\ [c] &= [\phi]^T[C][\phi] \quad - \quad \textit{modal damping matrix} \\ [m] &= [\phi]^T[M][\phi] \quad - \quad \textit{modal mass matrix} \\ \{f(t)\} &= [\phi]^T\{F(t)\} \quad - \quad \textit{modal load vector}. \end{aligned} \tag{57}$$

The matrices $[k]$ and $[m]$ are diagonal, while $[c]$ becomes diagonal only in a special case, for instance if $[C] = \alpha_0\,[M] + \beta_0\,[K]$, where α_0 and β_0 are coefficients [20].

Solving (56) for undamped natural vibration, $[k]=[\omega^2 m]$ is obtained, and by its backward substitution into (56) the final form of the modal equation yields

$$\left[\omega^2\right]\{X\}+2[\omega][\zeta]\{\dot{X}\}+\left\{\ddot{X}\right\} = \{\varphi(t)\}, \tag{58}$$

where

$$\begin{aligned} [\omega] &= \left[\sqrt{\frac{k_{ii}}{m_{ii}}}\right] \quad -- \textit{ natural frequency matrix} \\ [\zeta] &= \left[\frac{c_{ij}}{2\sqrt{(k_{ii}m_{ii})}}\right] \quad -- \textit{ relative damping matrix} \\ \{\varphi(t)\} &= \left\{\frac{f_i(t)}{m_{ii}}\right\} \quad -- \textit{ relative load vector}. \end{aligned} \tag{59}$$

If $[\zeta]$ is diagonal, the matrix Eq. (58) is split into a set of uncoupled modal equations.

The ship vibration is caused by the engine and propeller excitation forces, which are of periodical nature and therefore can be split into harmonics. Thus, the ship's hull response is obtained solving either (51) or (56). In both cases, the system of differential equations is transformed into a system of algebraic equations.

If hull vibration is induced by waves, the time integration of (51) or (56) has to be performed. Several numerical methods are available for this purpose, as for instance the Houbolt, the Newmark and the Wilson θ method [21], as well as the harmonic acceleration method [22,23].

It is important to point out that all stiffness and mass matrices of the beam finite element (and consequently those of the assembly) are frequency dependent quantities, due to coefficients α and η in the formulation of the shape functions, Eqs. (34) and (35). Therefore, for solving the eigenvalue problem (53) an iteration procedure has to be applied. As a result of frequency dependent matrices, the eigenvectors are not orthogonal. If they are used in the modal superposition method for ship hydroelastic analysis, full modal stiffness and mass matrices (as those of added mass and hydrodynamic damping) are generated. Since the inertia terms are much smaller than the deformation ones in Eqs. (24) and (25), the off-diagonal elements in modal stiffness and mass matrices are very small compared to the diagonal elements and can be neglected.

It is obvious that the usage of the physically consistent non-orthogonal natural modes in the modal superposition method is not practical, especially not in the case of time integration. Therefore, it is preferable to use mathematical orthogonal modes for that purpose. They are created by the static displacement relations yielding from Eqs. (24) and (25) with $\omega = 0$, that leads to $\alpha = \eta = 1$. In that case all finite element matrices, defined with Eqs. (37) and in Appendix B, can be transformed into explicit form, Appendix D. The resulting discrepancies of these two different formulations are analysed analytically in Appendix E and numerically within the following illustrative example.

6. Particulars of container ship

The application of the improved theory and numerical procedure is illustrated in case of an 11400 TEU VLCS (Very Large Container Ship), Fig. 4. The main vessel particulars are the following:

Length overall, $L_{oa}=363.44$ m
Length between perpendiculars, $L_{pp}=348$ m
Breadth, $B=45.6$ m
Depth, $H=29.74$ m
Draught, $T=15.5$ m
Displacement, full load, $\Delta_f=171445$ t
Displacement, ballast, $\Delta_b=74977$ t
Displacement, lightweight, $\Delta_l=37151$ t
Engine power, $P=72240$ kW
Ship speed, $v=24.7$ kn

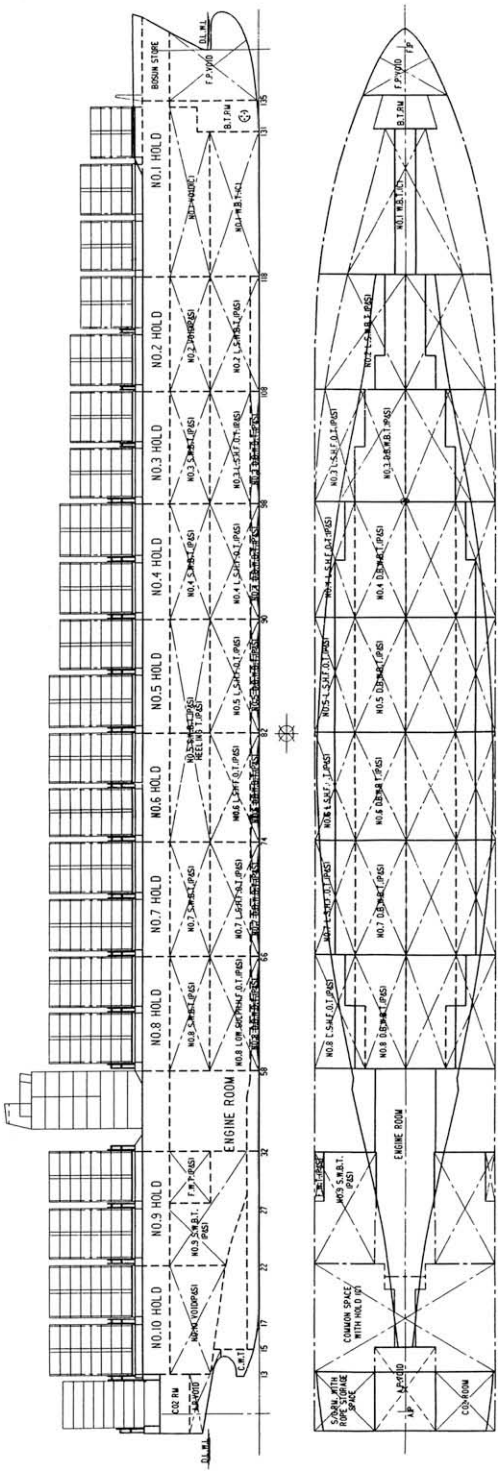

Fig. 4. 11400 TEU container ship.

The midship section, which shows a double skin structure with the web frames and longitudinals, is presented in Fig. 5. The ship hull stiffness properties are calculated by the program STIFF [24], based on the theory of thin-walled girders [14,25], Appendix F. Their distributions along the ship are shown in Fig. 6. It is evident that geometrical properties rapidly change values in the engine and superstructure area, due to closed ship cross-section. This is especially pronounced in the case of torsional modulus, which takes quite low values for the open cross-section and rather high values for the closed one, Fig. 6e. Novelty is the distribution of the shear inertia modulus I_s, Fig. 6f. Bulkhead influence is taken into account by increasing the value of the torsional modulus $I_t^* = 1.9I_t$ as it is elaborated in Appendix G.

Dry vibration analysis is performed for the lightweight loading condition. The containers are excluded from the analysis since they influence only the mass properties while the structural model is of primary interest. Ship mass distribution and its properties are shown in Fig. 7. The mass bimoment of inertia J_w is neglected due to its very small influence on vibrations.

7. 1D vibration analysis

Dry natural vibrations are calculated by the modified and improved program DYANA within [4]. The ship hull is divided into 50 beam finite elements. Finite elements of closed cross-section (6 d.o.f., ϑ excluded) are used in the ship bow, ship aft and in the engine room area. First, natural frequencies of horizontal vibrations are calculated by the finite element with consistent frequency dependent and independent properties, as well as for the case of no mass rotation Table 1. Relations between the results are similar to those noticed in the analytical evaluation of the approximate solution in Appendix E. Negligible small discrepancies between natural frequencies of the mathematical and physical modes are evident. Influence of mass rotation on frequencies is within 4%. So, the mathematical natural modes determined by finite elements with frequency independent shape functions are very reliable to be used in the ship hydroelastic analysis.

The first five natural frequencies for vertical and horizontal vibrations are listed in Tables 2 and 3 for further analysis. The corresponding natural modes are of ordinary shapes. Natural frequencies of coupled horizontal and torsional vibrations are listed in Table 4. The first five natural modes presented by the twist angle, ψ, and the hull deflection at the level of center of gravity, w_G, are shown in Fig. 8. These functions are mutually dependent. However, they are normalized by their own maximum values due to a simpler presentation. There always occurs coupling between frequency close symmetric flexural and torsional modes as well as anti-symmetric ones [26,27]. This is indicated in Table 4, where the 5th coupled mode is an extraordinary natural mode comprised of the 2nd torsional and the 5th flexural elementary modes.

Once the dry natural modes of ship hull are determined, it is possible to transfer the beam node displacements to the ship wetted surface for the hydrodynamic calculation. The transformation (spreading) functions for vertical and coupled horizontal and torsional vibration yield respectively [3]

$$\mathbf{h}_v = -\frac{\mathrm{d}w_v}{\mathrm{d}x}(Z - z_C)\mathbf{i} + w_v\mathbf{k} \tag{60}$$

$$\mathbf{h}_{ht} = \left(-\frac{\mathrm{d}w_h}{\mathrm{d}x}Y + \frac{\mathrm{d}\psi}{\mathrm{d}x}\overline{u}\right)\mathbf{i} + [w_h + \psi(Z - z_S)]\mathbf{j} - \psi Y\mathbf{k}, \tag{61}$$

where w is hull deflection, ψ is twist angle, $\overline{u} = \overline{u}(x, Y, Z)$ is the cross-section warping function reduced to the wetted surface, z_C and z_S are coordinates of centroid and shear centre respectively, and Y and Z are coordinates of the point on the ship surface. The first two dry natural modes of the ship wetted surface in case of vertical and coupled horizontal and torsional vibrations are shown in Figs. 9–12 respectively. In the latter case, the orthogonal view on the vertical and horizontal planes is used.

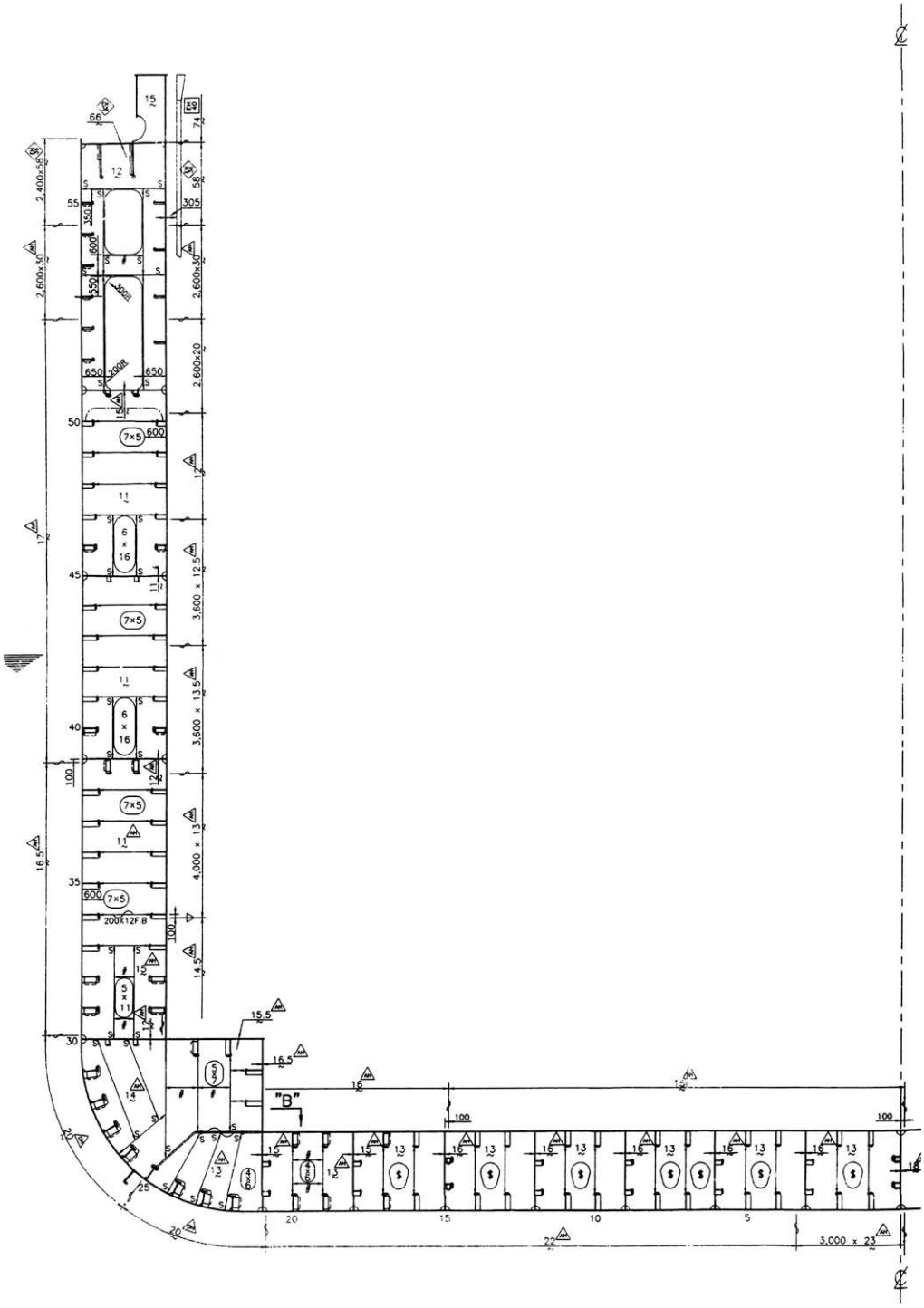

Fig. 5. Midship section.

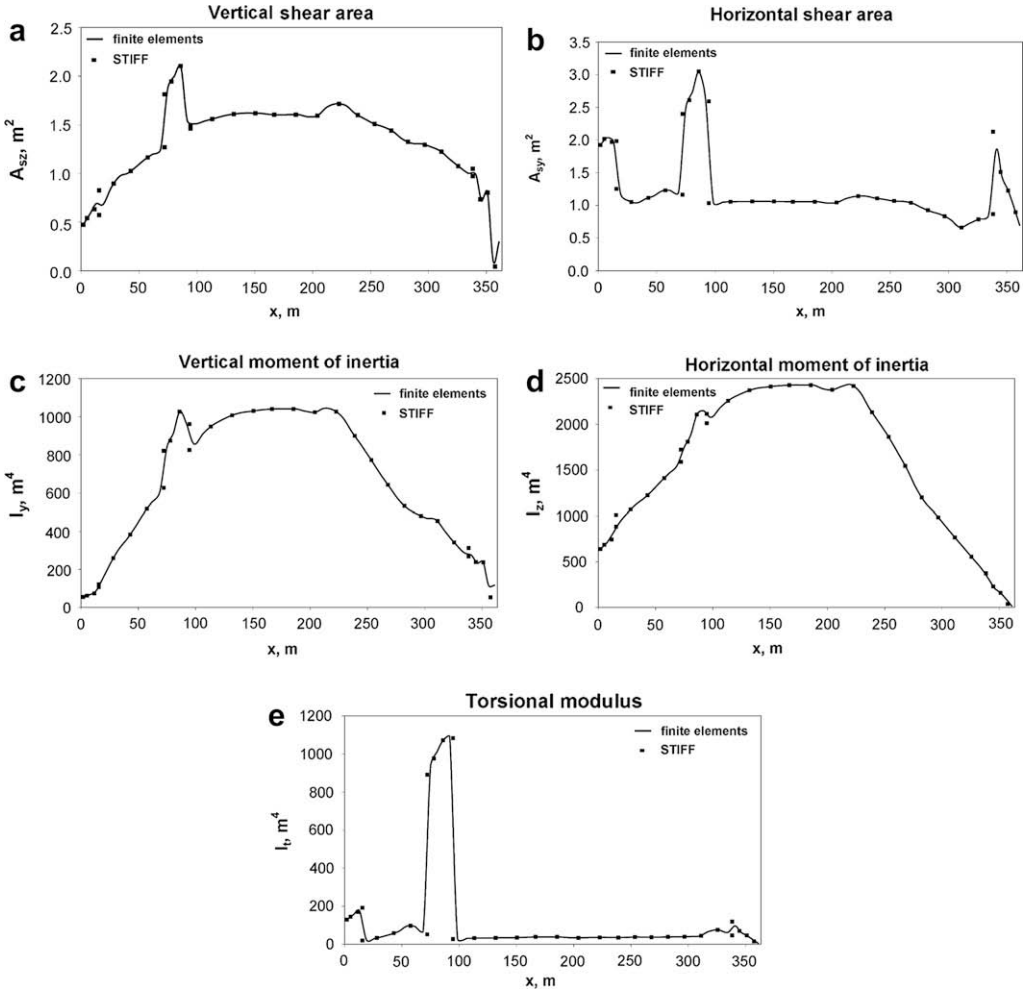

Fig. 6. Longitudinal distribution of ship cross-section geometrical properties.

8. 3D vibration analysis

For this purpose, a fine 3D FEM model of the container vessel is created by NASTRAN program [28]. The model includes 33072 nodes, 84076 finite elements (38288 shells and 45788 beams), and 187290 d.o.f. The ship mass distribution (steel and equipment) is given by adjusted mass density for the finite element blocks. Only the main engine mass is specified by the lumped masses. The Lanczos method is used for the solution of the eigenvalue problem.

In order to uncouple the horizontal vibrations from the torsional ones, for the purpose of a more detailed correlation analysis, the FEM model is reinforced by a set of vertical rigid massless beams in the longitudinal symmetry plane. The rotation of all beam nodes around axial axis is fixed.

Natural frequencies of vertical, horizontal and coupled horizontal and torsional vibrations are listed in Tables 2–4, respectively. The first five natural modes of the coupled vibrations, which are of primary interest, are shown in Figs. 13–17. The lateral and bird views are used in order to achieve easier recognition of the elementary modes in each coupled mode. We can see that in all vibration modes

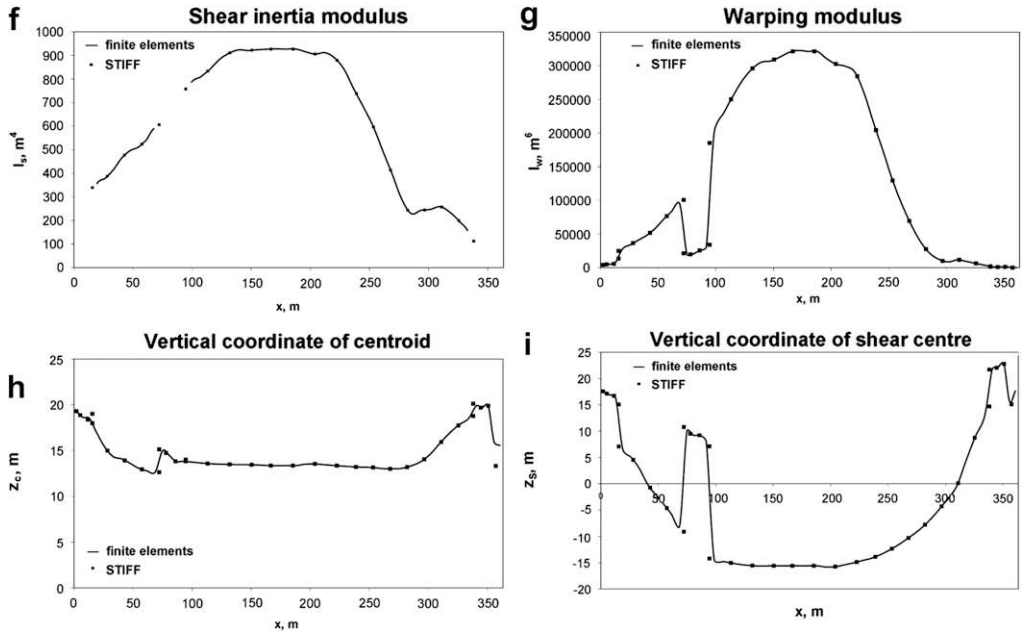

Fig. 6. (*continued*).

warping of the front (collision) bulkhead and the aft (transom) bulkhead is rather low. Thus, the assumption of restrained warping of hull peaks, introduced in 1D FEM model, is quite realistic.

9. Correlation analysis

It is possible to compare now the first two vibration modes determined by 1D and 3D FEM analyses, Figs. 11–14, respectively. The same mode shapes are obvious. Natural frequencies of vertical, horizontal and coupled horizontal and torsional vibrations determined by 1D and 3D FEM models are correlated in Tables 2–4, respectively, with indicated discrepancies. The general opinion concerning the accuracy of 1D vibration analysis is that the first five eigenpairs are acceptable from the engineering viewpoint, with frequencies tolerance discrepancy of up to 5%. In the considered case, the agreement of natural frequencies for vertical vibrations is quite good. Somewhat large discrepancies appear for the fifth frequency of horizontal vibration (8.78%). This discrepancy is magnified in the fifth frequency of the extraordinary coupled horizontal and torsional vibrations (16.81%), comprised of the 5th elementary horizontal mode and the 2nd torsional mode, Fig. 17.

It is necessary to point out that 1D eigenpairs are determined for the fixed ship stiffness and mass properties. However, if the mode dependent effective values of parameters are taken into account, discrepancies between 1D and 3D results are considerably reduced, and the validity of 1D vibration analyses can be extended up to the 10th mode. The effective stiffness parameters are determined by utilizing the strip element method and the energy approach [29]. The main idea is to specify the harmonic load distribution and the harmonic mode shapes and split the strain energy into normal and shear parts, and then to estimate the effective bending modulus and shear area based on the separated energies, Appendix H.

In order to illustrate the above fact, 1D vibration calculation is repeated, taking the mode dependent moment of inertia of cross-section, $I_{Z5} = i_5 I_Z$, and shear area, $A_{sy5} = a_5 A_{sy}$ into account. The roughly estimated values $i_5 = 0.2$ and $a_5 = 1.2$ are taken from the channel girder analysis, Fig. 18 [14]. Since deflection of a girder for higher modes is mainly due to shear, values of a_n are increased to some extent, while those of i_n asymptotically approach zero. The actual natural frequencies are compared in Table 5. It is obvious that the discrepancies between 1D and 3D results are now considerably reduced.

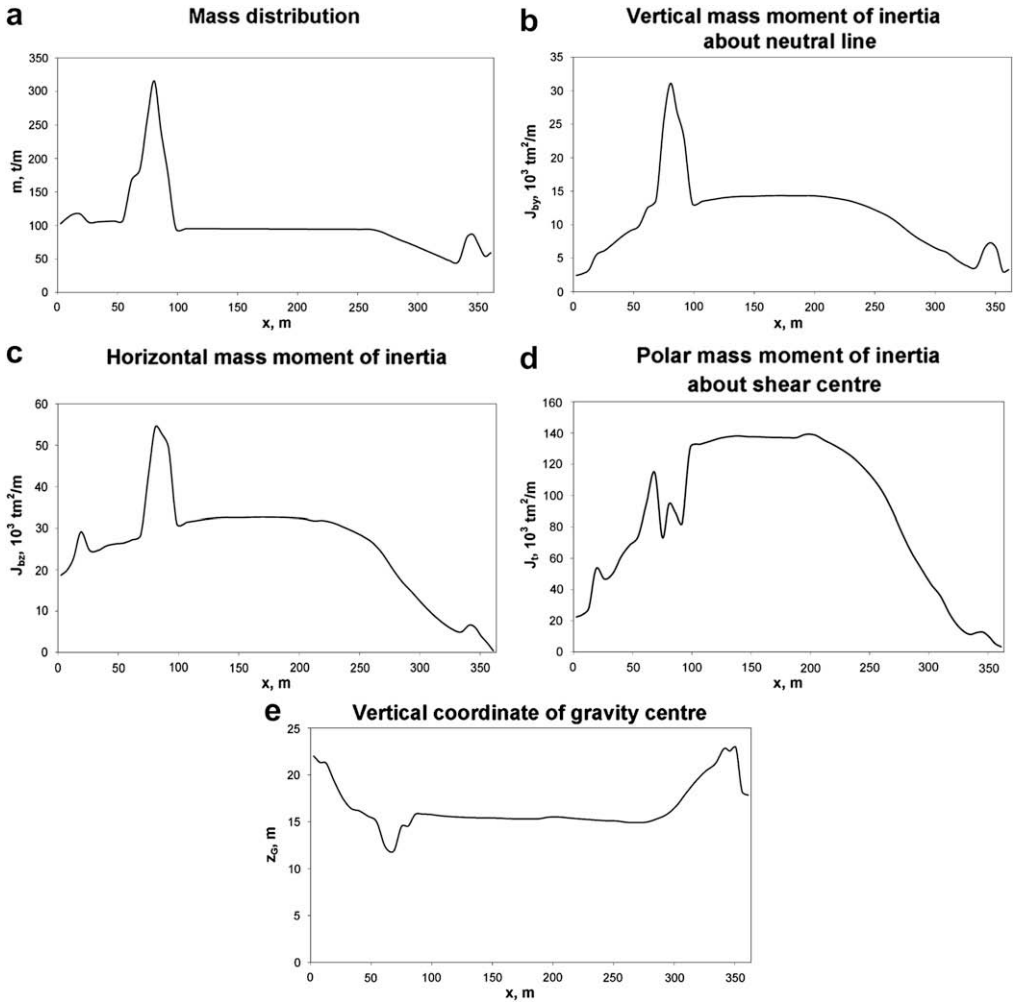

Fig. 7. Longitudinal distribution of ship mass properties, lightweight.

Table 1
Natural frequencies of horizontal hull vibrations, ω_i (Hz).

Mode no.	Physical mode, a	Mathematical mode, b	$J_{bz} = 0$, c	Discrepancy %	
				$b/a - 1$	$c/a - 1$
1	1.552	1.552	1.584	0	2.06
2	2.740	2.740	2.801	0	2.23
3	4.022	4.021	4.070	−0.02	1.19
4	5.697	5.694	5.743	−0.05	0.08
5	7.398	7.392	7.483	−0.08	1.15
6	8.451	8.444	8.766	−0.08	3.73
7	9.569	9.557	9.802	−0.13	2.43
8	11.370	11.359	11.469	−0.10	0.87
9	13.352	13.329	13.115	−0.17	−1.81
10	14.490	14.453	14.311	−0.26	−2.56

Table 2
Natural frequencies of vertical hull vibrations, ω_i (Hz).

Mode no.	1D FEM	3D FEM	Discrepancy %
1	1.149	1.159	−0.86
2	2.318	2.327	−0.39
3	3.695	3.654	1.12
4	5.457	5.409	0.89
5	6.913	6.605	4.66

Table 3
Natural frequencies of horizontal hull vibrations, ω_i (Hz).

Mode no.	1D FEM	3D FEM	Discrepancy %
1	1.552	1.625	−4.49
2	2.740	2.787	−1.69
3	4.021	4.018	0.10
4	5.694	5.505	3.49
5	7.392	6.798	8.78

Table 4
Natural frequencies of coupled horizontal and torsional hull vibrations, ω_i (Hz).

Mode no.	Coupled modes	1D FEM	3D FEM	Discrepancy %
1	T1	0.639	0.638	0.16
2	T2 + H1	1.056	1.076	−1.86
3	T3 + H2	1.745	1.749	−0.23
4	T4 + H3	2.233	2.429	−8.07
5	T2 + H5	3.072	2.630	16.81
6	T5 + H4	3.350	3.519	−4.80

The 5th natural mode determined by 1D FEM model with the mode dependent stiffnesses is shown in Fig. 19. Changes of functions w_G and ψ are noticeable especially in the area of engine room. The new mode shape is now closer to the 3D one, Fig. 17, than that shown in Fig. 8e.

Zoom of the deformed ship aftbody in case of the 5th mode vibrations, is shown in Fig. 20. Warping of the transverse bulkheads is quite pronounced in this mode. The engine room structure is rather stiff concerning bending, while there is some warping release of its bulkheads. The warping magnitude in the beam model is represented by variation of twist angle ϑ. Its given value is zero within the engine room as well as hull peaks, due to closed cross-sections, Fig. 19. It is quite difficult to simulate the local warping effect in the engine room by 1D FEM model.

In 1D vibration analysis we distinguish the so-called mathematical natural modes and the actual physical modes, determined by fixed and mode dependent vibration properties, respectively. The former modes are mutually orthogonal and therefore suitable to be used as the coordinate functions for determining structural forced response by the modal superposition method. As result of that property, the diagonal modal stiffness and mass matrices are generated. Consequently, the modal equations are weakly coupled only by the modal damping. Thus, the equations can be easily solved by an iteration procedure.

The application of the actual physical vibration modes, i.e. those determined with the effective values of vibration parameters, in the modal superposition method is not suitable due to coupling of modal equations as a result of mode non-orthogonality, Appendix H. This is anyway out of interest in case of ship hydroelasticity analysis, since the ship structure response to waves occurs in the lower frequency domain and is successfully described by the first few natural modes only. In the frequency domain the mathematical modes are rather close to the actual ones, and it does not matter which are used in the modal superposition method. The calculated ship response will be the same in both cases.

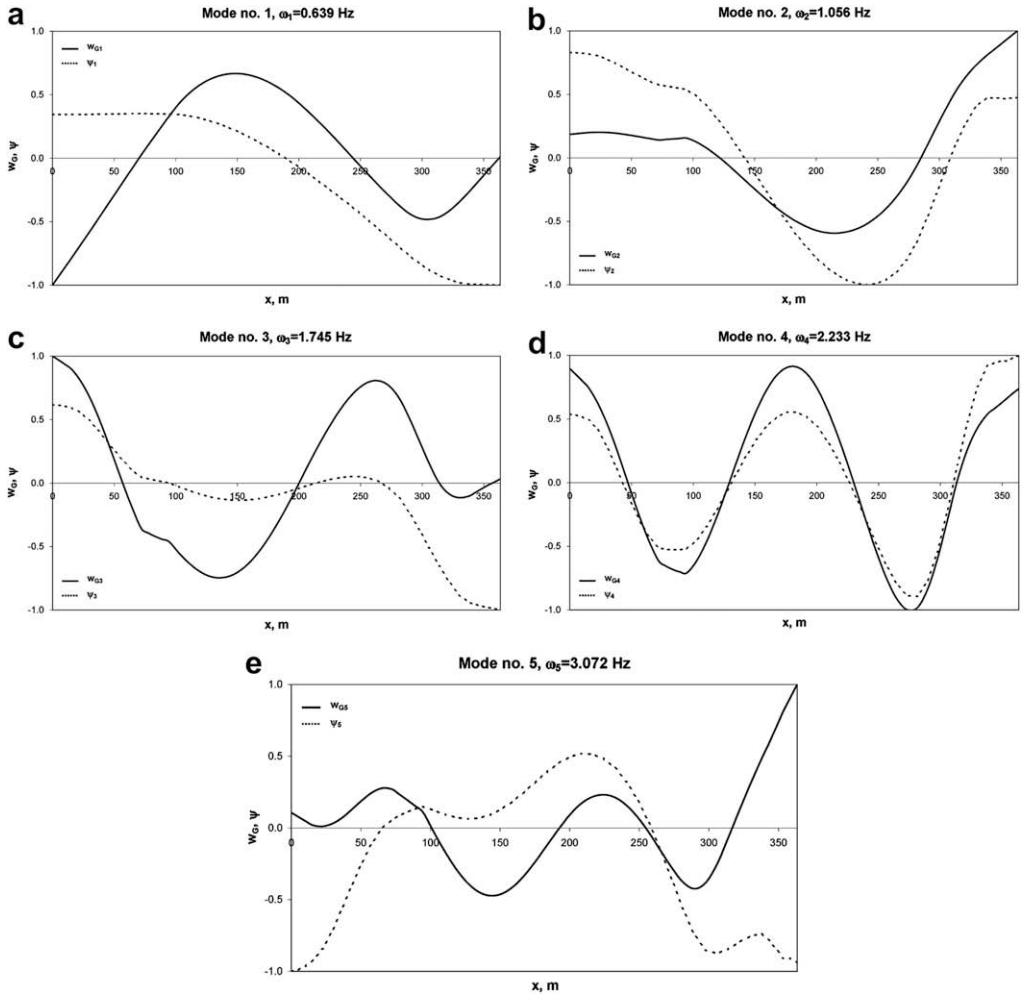

Fig. 8. Natural modes of coupled horizontal and torsional vibrations, 1D model.

10. Conclusion

Very large container ships are quite flexible and their design and construction are at the margin of the present classification rules. Therefore, great effort is done nowadays to investigate the ship hydroelasticity phenomenon. Dry natural vibration analysis, utilizing either 1D or 3D FEM model, is the first step in solving this challenging problem. For the research purpose and preliminary design stage, the beam analysis combined with thin-walled girder theory is more suitable and convenient. It makes it possible to investigate the influence of all stiffness and mass parameters on ship dynamic behaviour and at the same time reduces the amount of work needed to carry out the analysis.

In order to increase the reliability of thin-walled girder theory some improvement of the classical theory is proposed. Shear influence on torsion is included in the theoretical consideration by following analogy between bending and torsion. Shear influence is more pronounced in torsion than in bending. The beam finite element for coupling flexural and torsional vibrations is developed with complete stiffness and mass matrices. Two approaches are used, the consistent frequency dependent shape functions, and frequency independent ones, which follows from static beam theory. It is shown that discrepancies between the vibration results are negligible. Also, the influence of

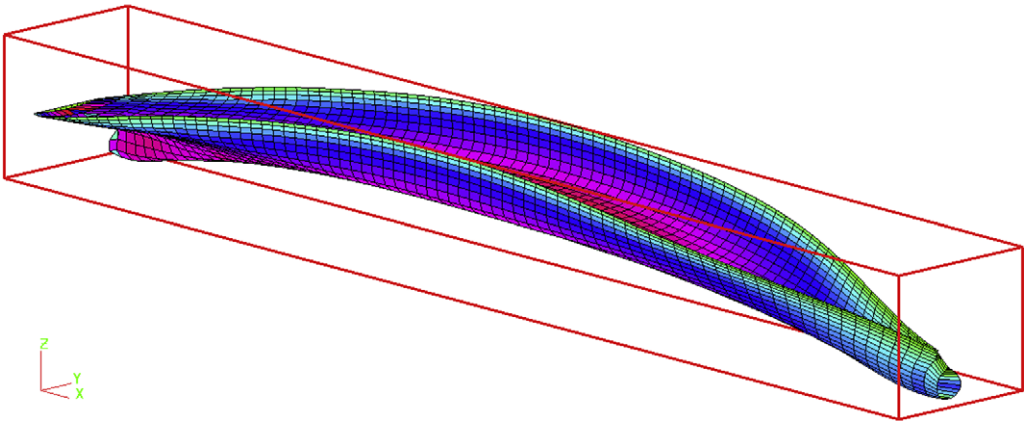

Fig. 9. The first natural mode of vertical vibrations, $\omega_1 = 1.149$ Hz, 1D model.

transverse bulkheads is incorporated in the hull torsional stiffness, based on detailed determination of the bulkhead strain energy as an orthotropic plate with rigid stool.

The developed procedure is illustrated in case of a very large container ship and the accuracy of the results is verified by the correlation analysis with the results from 3D FEM analysis. By taking all relevant ship stiffness and mass parameters into account, quite good agreement of the results is achieved in the low frequency domain. The application of the beam model for ship hull vibrations is limited to the first five natural modes. However, this is sufficient for the ship hydroelasticity analysis since the most energy of wave spectrum is concentrated in the low frequency domain, i.e. below natural frequency of the first elastic mode of the ship hull.

The 3D FEM analysis shows that the assumption on restrained warping in the ship peaks is realistic. However, in spite of the fact that the engine room is a closed cross-section substructure, some warping release is noticed in case of extraordinary and higher natural modes. The present solutions in the literature, as for instance that shown in [11], which is correlated to a simplified one in [30], are not very promising. Therefore, this problem requires further investigation and incorporation in the beam model. The basic idea is to consider engine room structure as an open cross-section segment with week deck and platforms and determine effective torsional, warping and shear moduli utilizing the energy approach.

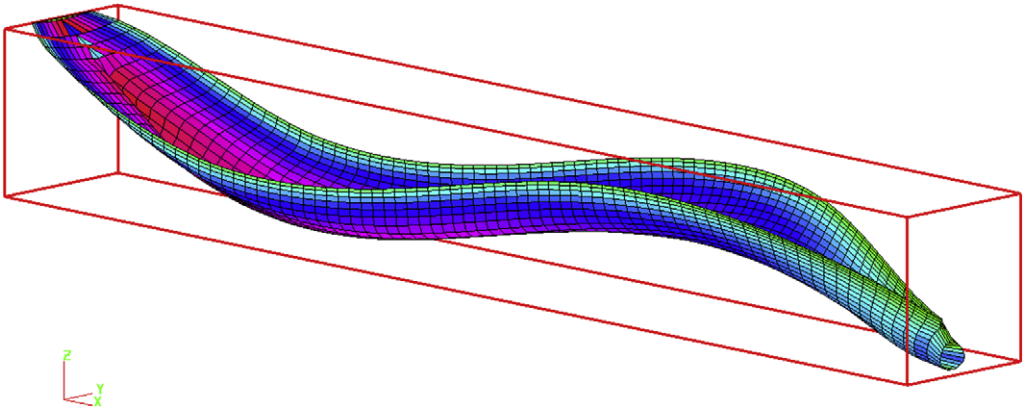

Fig. 10. The second natural mode of vertical vibrations, $\omega_2 = 2.318$ Hz, 1D model.

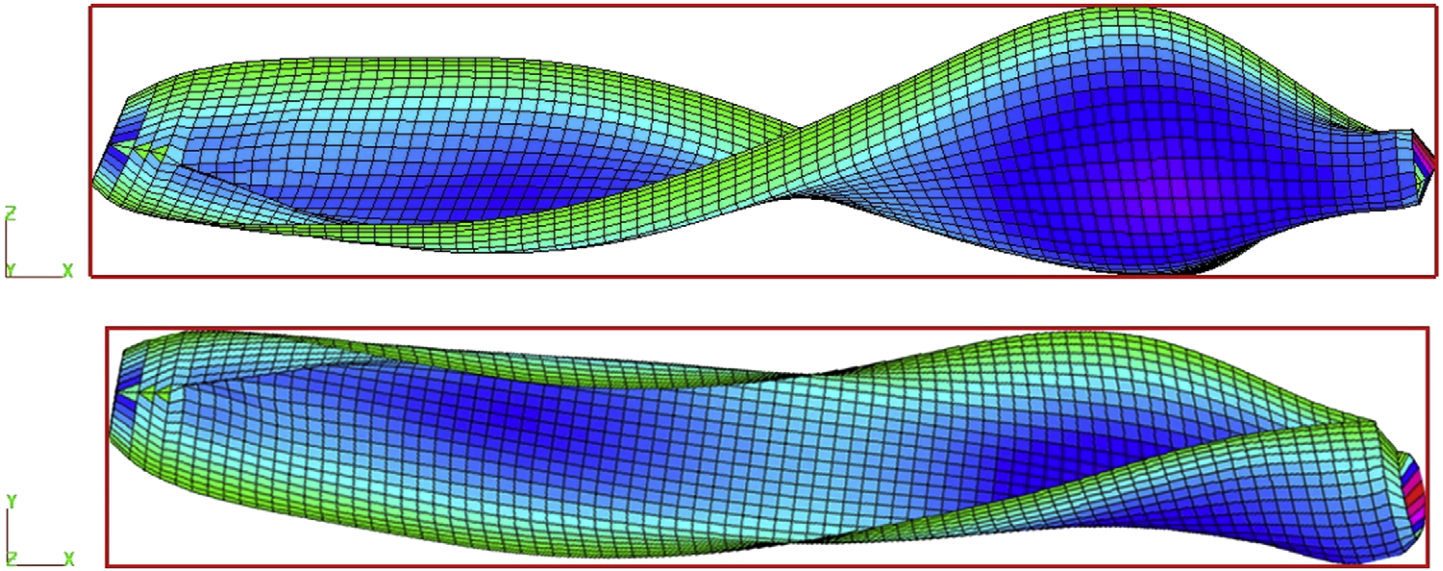

Fig. 11. The first natural mode of coupled horizontal and torsional vibrations, $\omega_1 = 0.639$ Hz, 1D model.

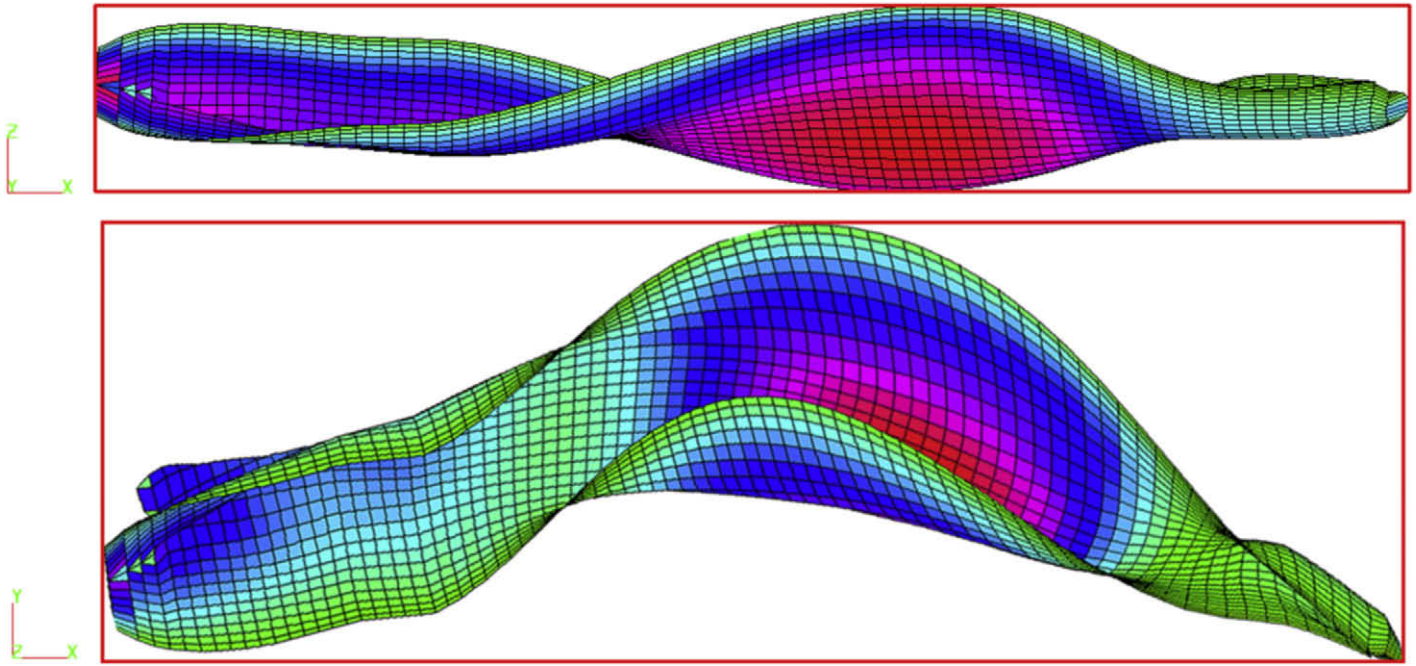

Fig. 12. The second natural mode of coupled horizontal and torsional vibrations, $\omega_2 = 1.056$ Hz, 1D model.

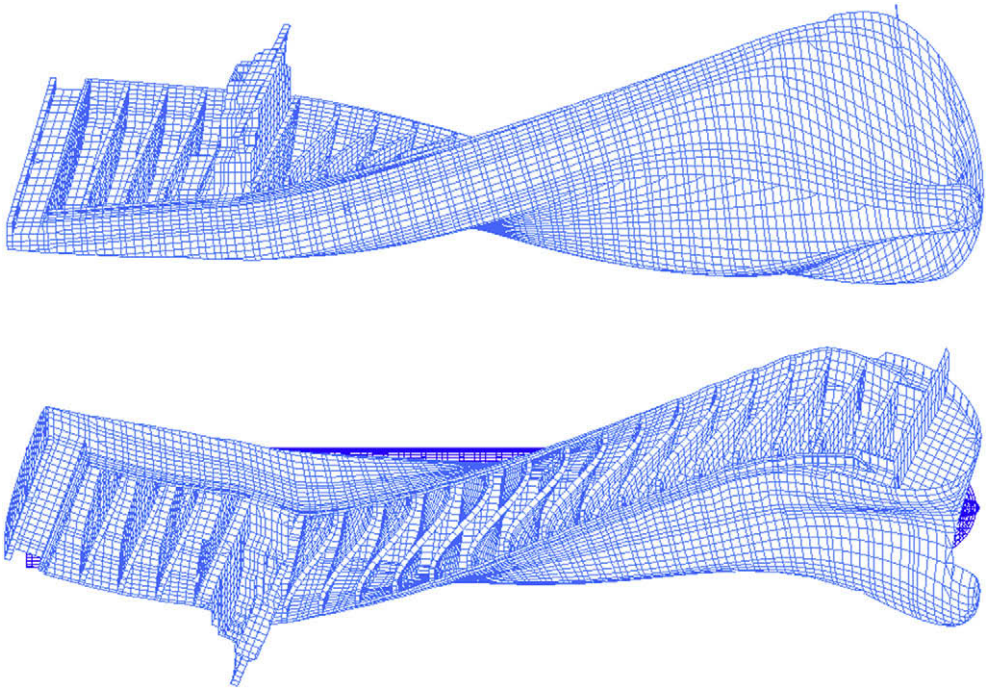

Fig. 13. The first natural mode of coupled horizontal and torsional vibrations, $\omega_1 = 0.638$ Hz.

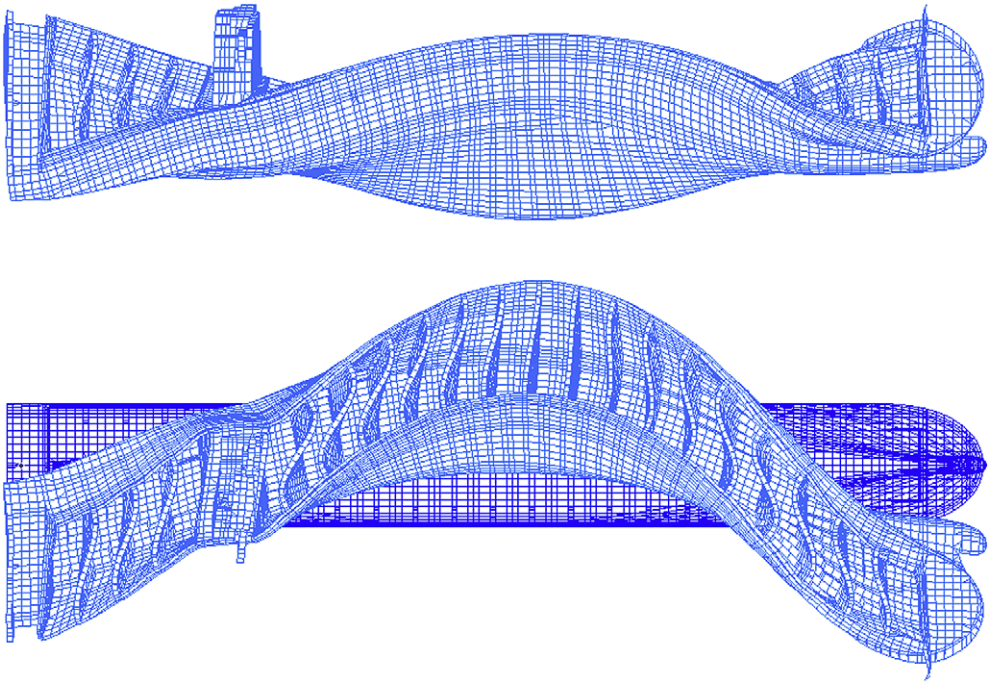

Fig. 14. The second natural mode of coupled horizontal and torsional vibrations, $\omega_2 = 1.076$ Hz.

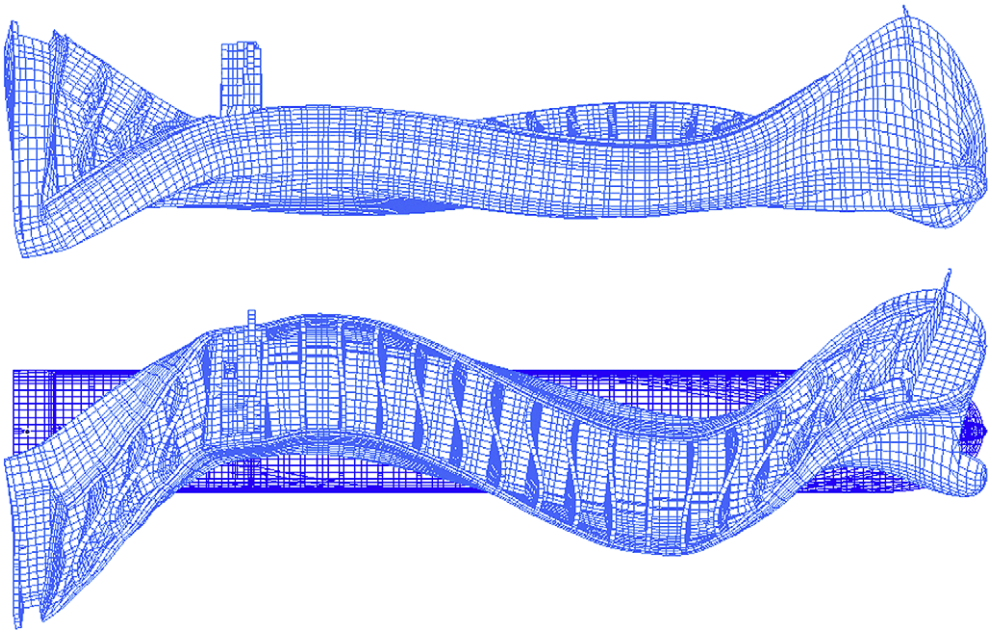

Fig. 15. The third natural mode of coupled horizontal and torsional vibrations, $\omega_3 = 1.749$ Hz.

The beam model of ship hull presented in this paper is reliable enough to be directly applied in ship hydroelastic analyses. The most discrepancies between 1D and 3D model are reduced by taking shear influence on torsion as an additional stiffness parameter into account, as well as by incorporating transverse bulkhead stiffness contribution in a very efficient way.

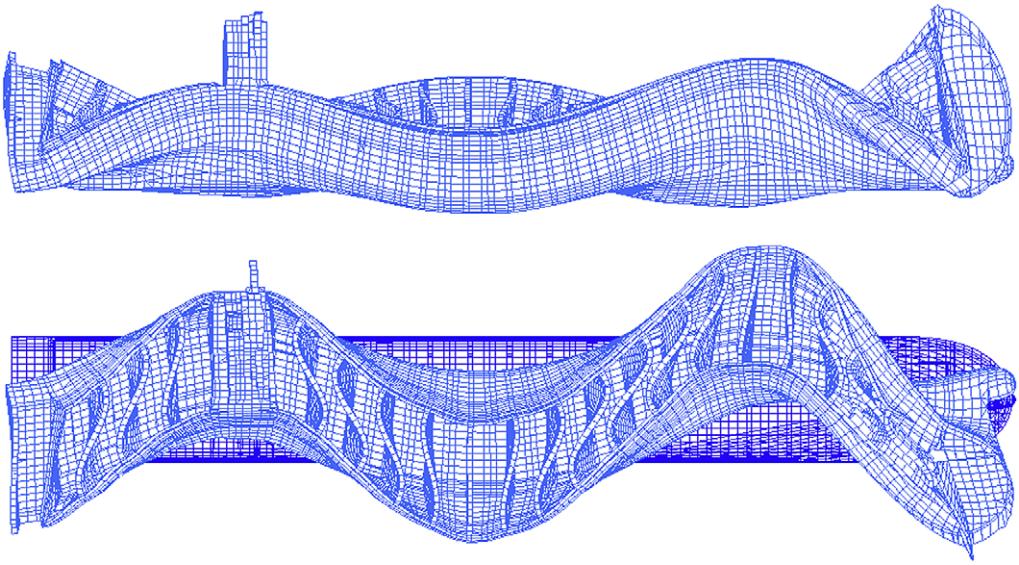

Fig. 16. The fourth natural mode of coupled horizontal and torsional vibrations, $\omega_4 = 2.429$ Hz.

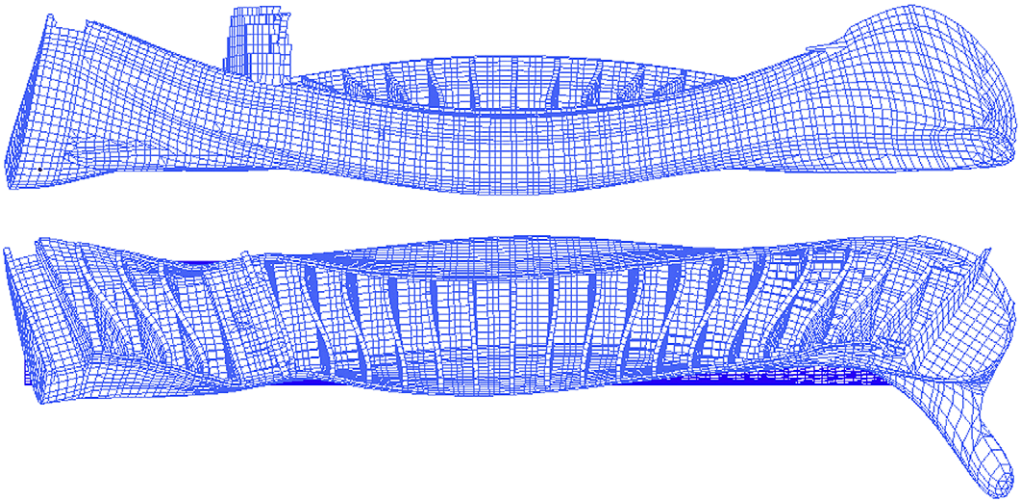

Fig. 17. The fifth natural mode of coupled horizontal and torsional vibrations, $\omega_5 = 2.630$ Hz.

Further improvement of the beam model, insisting on the consistence of compatibility conditions at joints of open and closed cross-section hull segments will have very small influence on global sectional forces of ship hull. In any case, beam model cannot get proper stress concentration in the deck corners for fatigue analysis. Therefore, it is necessary to employ the substructure technique, imposing sectional forces at substructure boundaries.

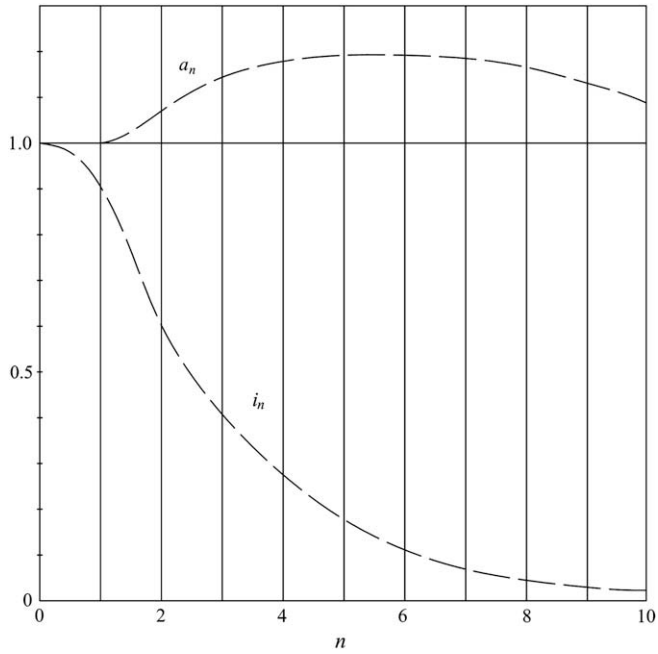

Fig. 18. Efficiency factors of horizontal bending modulus and shear area of channel girder i_n, a_n.

Table 5
The 5th natural frequencies, ω_5 (Hz), $I_{Z5} = 0.2I_Z$, $A_{Sy5} = 1.2A_{Sy}$.

	1D FEM	3D FEM	Discrepancy %
Horizontal	7.018	6.798	3.24
Coupled	2.747	2.630	4.45

Acknowledgment

This research was supported by the Ministry of Science, Education and Sport of the Republic of Croatia (Project No. 120-1201703-1704). The authors would like to express their gratitude to Ms. Estelle Stumpf, research engineer at Bureau Veritas, Marine Division – Research Department, for generating 3D FEM model of the container ship.

Appendix A. Torsional vibrations of prismatic beam

In order to analyse influence of stiffness and mass parameters on torsional vibrations, the natural vibrations of a prismatic beam are considered. The governing differential equation of motion is deduced from (21) by neglecting distance between center of gravity and shear center, $c = 0$, and warping bimoment of inertia, $J_w = 0$, due to reason of simplicity.

$$EI_w \frac{\partial^4 \psi_t}{\partial x^4} - GI_t \frac{\partial^2 \psi_t}{\partial x^2} + J_t^0 \left(\frac{\partial^2 \psi_t}{\partial t^2} - \frac{EI_w}{GI_s} \frac{\partial^4 \psi_t}{\partial x^2 \partial t^2} \right) = 0. \tag{A1}$$

Since natural vibrations are harmonic Eq. (A1) leads to the ordinary differential equation

$$EI_w \frac{d^4 \psi_t}{dx^4} - GI_t \left(1 - \omega^2 J_t^0 \frac{EI_w}{GI_t GI_s} \right) \frac{d^2 \psi_t}{dx^2} - \omega^2 J_t^0 \psi_t = 0, \tag{A2}$$

where ψ_t and ω are natural mode and frequency, respectively.

Solution of (A2) is assumed in the exponential form

$$\psi_t = e^{\alpha x}, \tag{A3}$$

and by substituting it in (A2) one finds the biquadratic characteristic equation

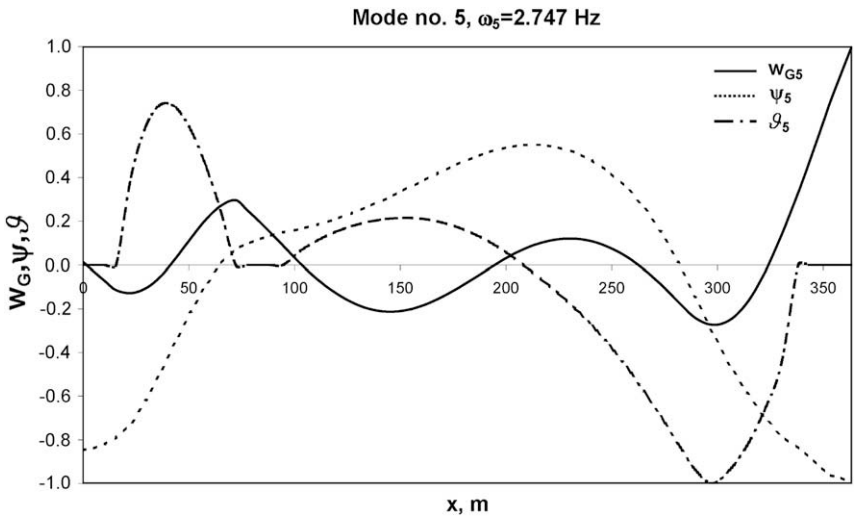

Fig. 19. The 5th natural mode of 1D FEM model, effective parameters $I_{Z5} = 0.2I_Z$ and $A_{Sy5} = 1.2A_{Sy}$.

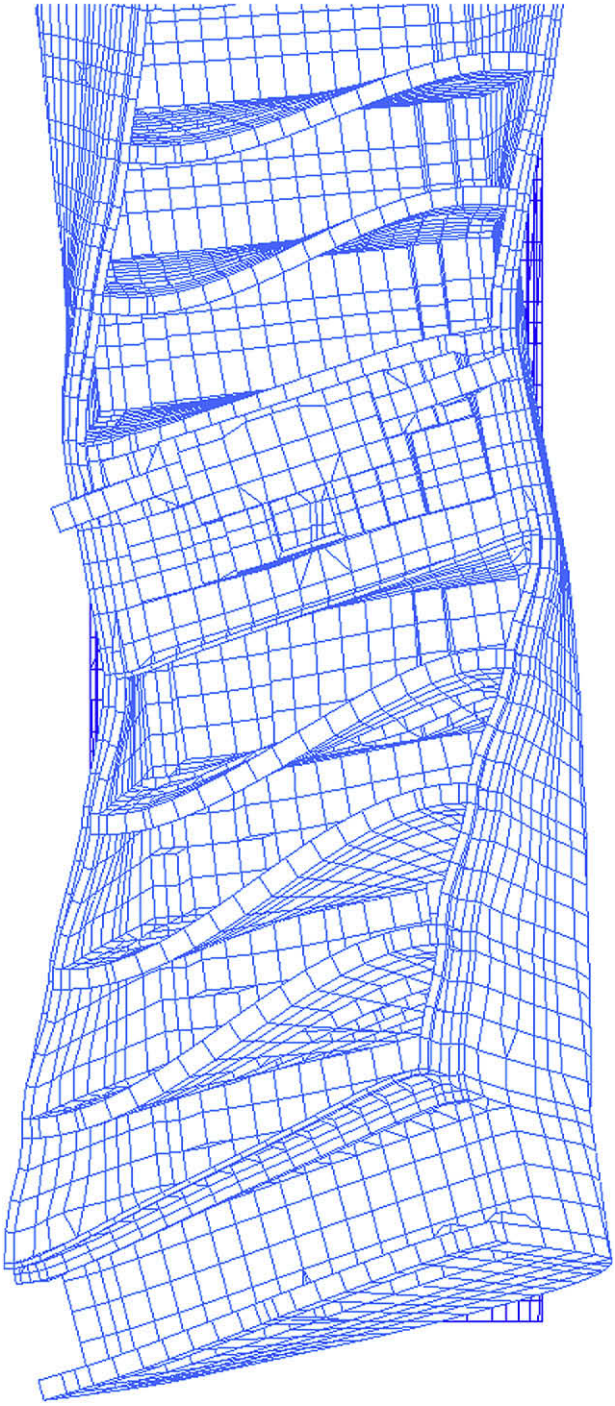

Fig. 20. Bird view of ship aftbody, the 5th natural mode.

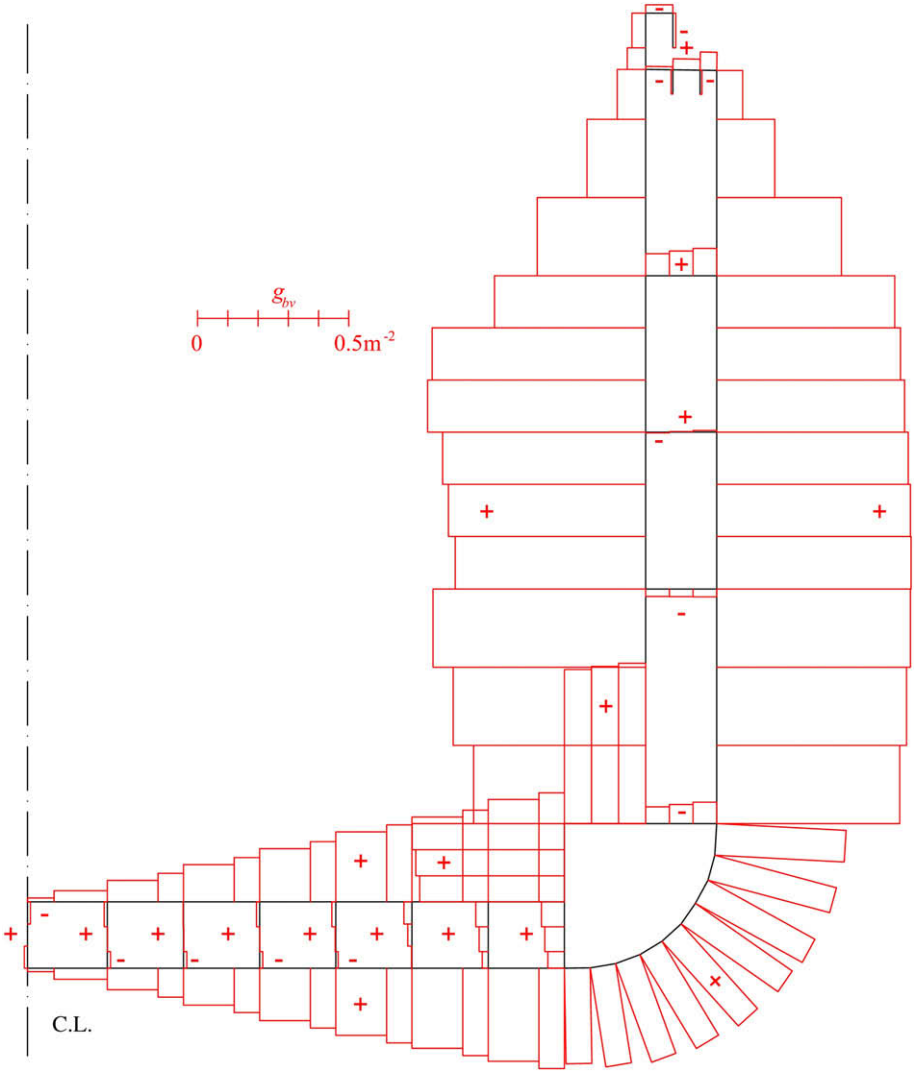

Fig. F1. Shear stress flow due to vertical bending.

$$\alpha^4 + b\alpha^2 + c = 0, \tag{A4}$$

where

$$b = \frac{GI_t}{EI_w}\left(\omega^2 J_t^0 \frac{EI_w}{GI_t GI_s} - 1\right), \quad c = -\frac{\omega^2 J_t^0}{EI_w}. \tag{A5}$$

Solutions of (A4) read

$$\alpha_j = \pm\eta, \ \pm i\chi, \tag{A6}$$

where

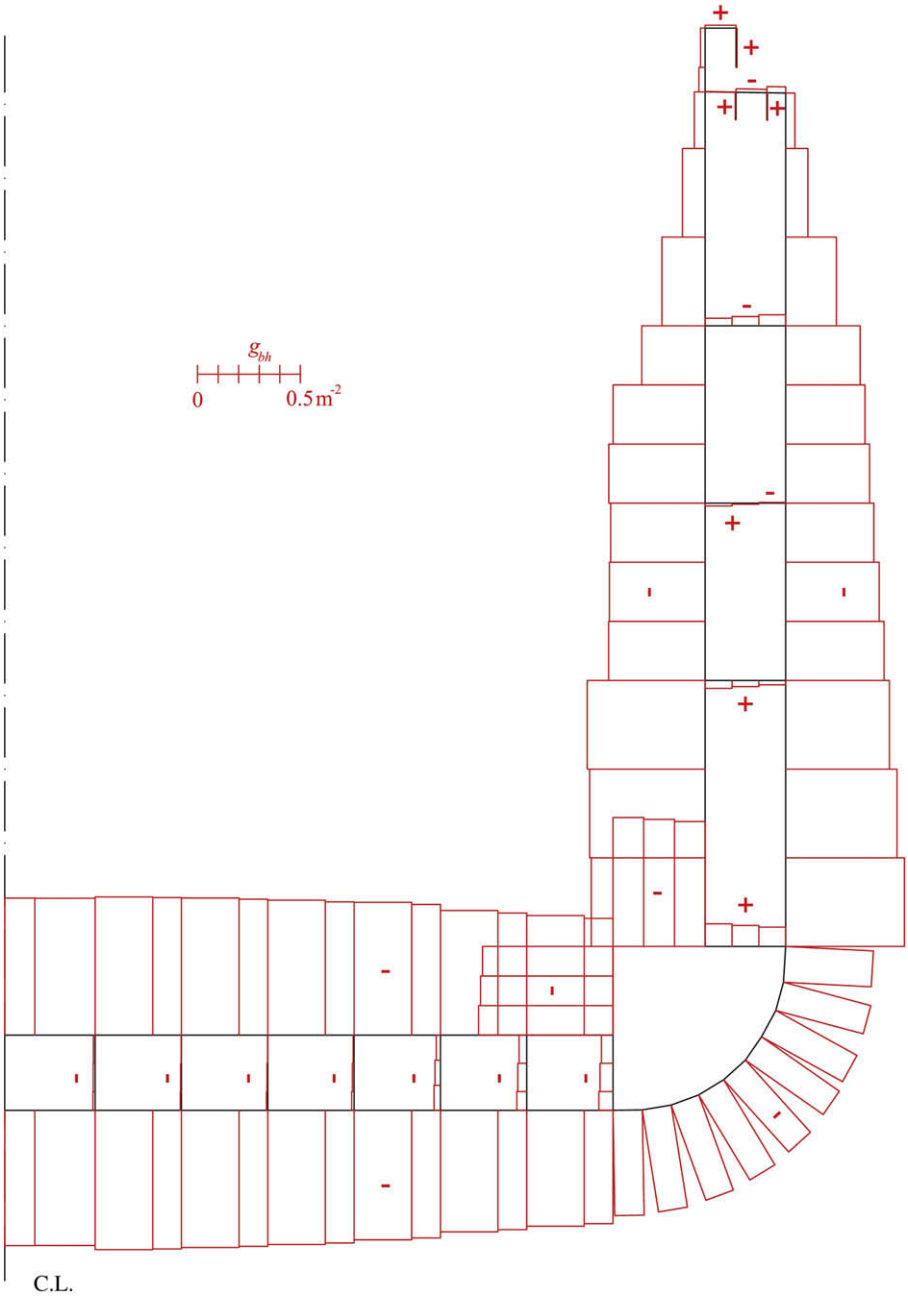

Fig. F2. Shear stress flow due to horizontal bending.

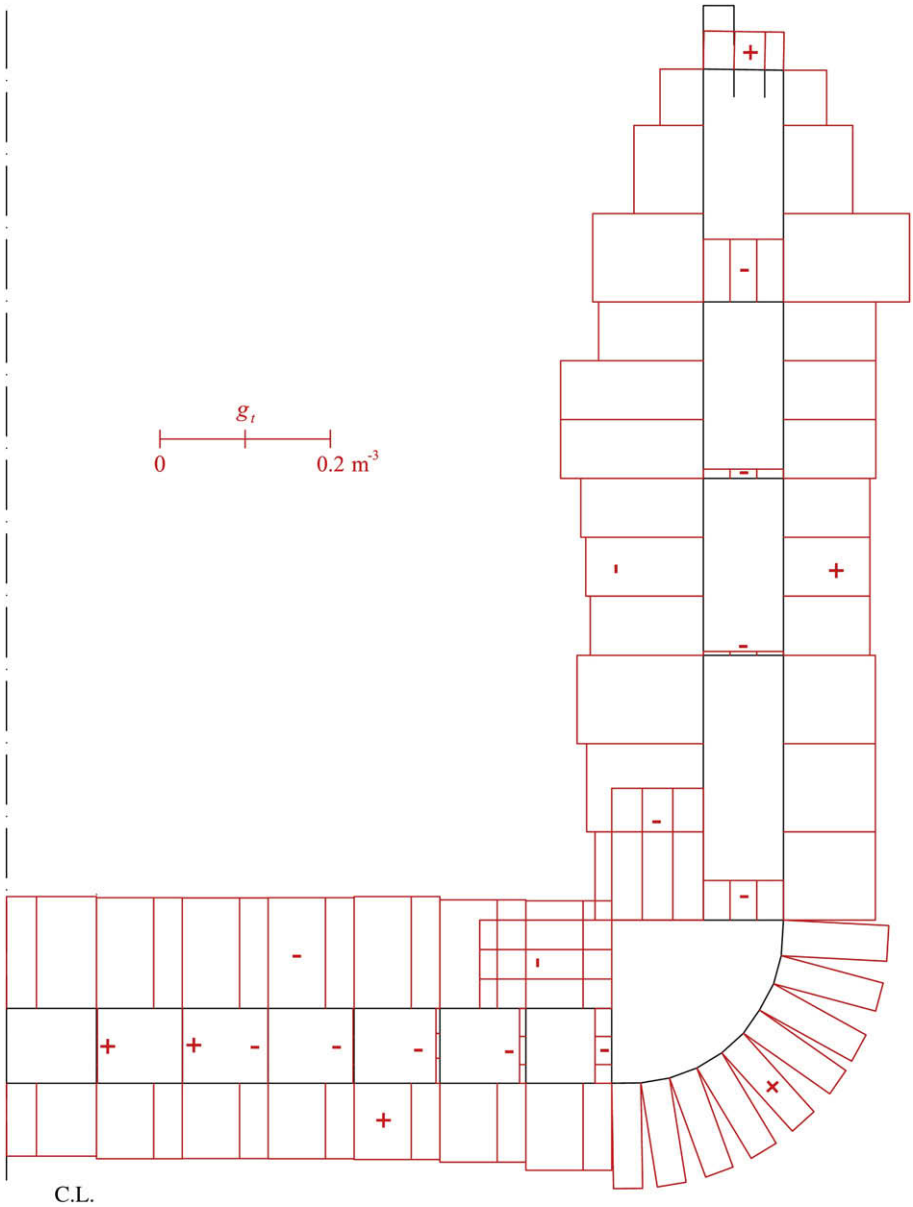

Fig. F3. Shear stress flow due to torsion.

$$\eta = \frac{1}{\sqrt{2}}\sqrt{\sqrt{b^2-4c}-b}, \chi = \frac{1}{\sqrt{2}}\sqrt{\sqrt{b^2-4c}+b}. \tag{A7}$$

Thus, solution of (A2) takes the form

$$\psi_t = A_1 sh\eta x + A_2 ch\eta x + A_3 \sin\chi x + A_4 \cos\chi x. \tag{A8}$$

Let us consider vibrations of a free beam of length $2l$, with restrained warping, $u = \bar{u}\vartheta$, at its ends. The relevant boundary conditions read

$$x = \pm l : T = 0, \ u = 0 \tag{A9}$$

that leads to

$$x = \pm l : \frac{d\psi_t}{dx} = 0, \ \frac{d^3\psi_t}{dx^3} = 0. \tag{A10}$$

In the case of symmetric modes $A_1 = A_3 = 0$, while for anti-symmetric modes $A_2 = A_4 = 0$. The corresponding eigenvalue problems yield

$$\begin{bmatrix} \eta sh\eta l & -\chi sin\chi l \\ \eta^3 sh\eta l & \chi^3 sin\chi l \end{bmatrix} \begin{Bmatrix} A_2 \\ A_4 \end{Bmatrix} = \{0\}, \tag{A11}$$

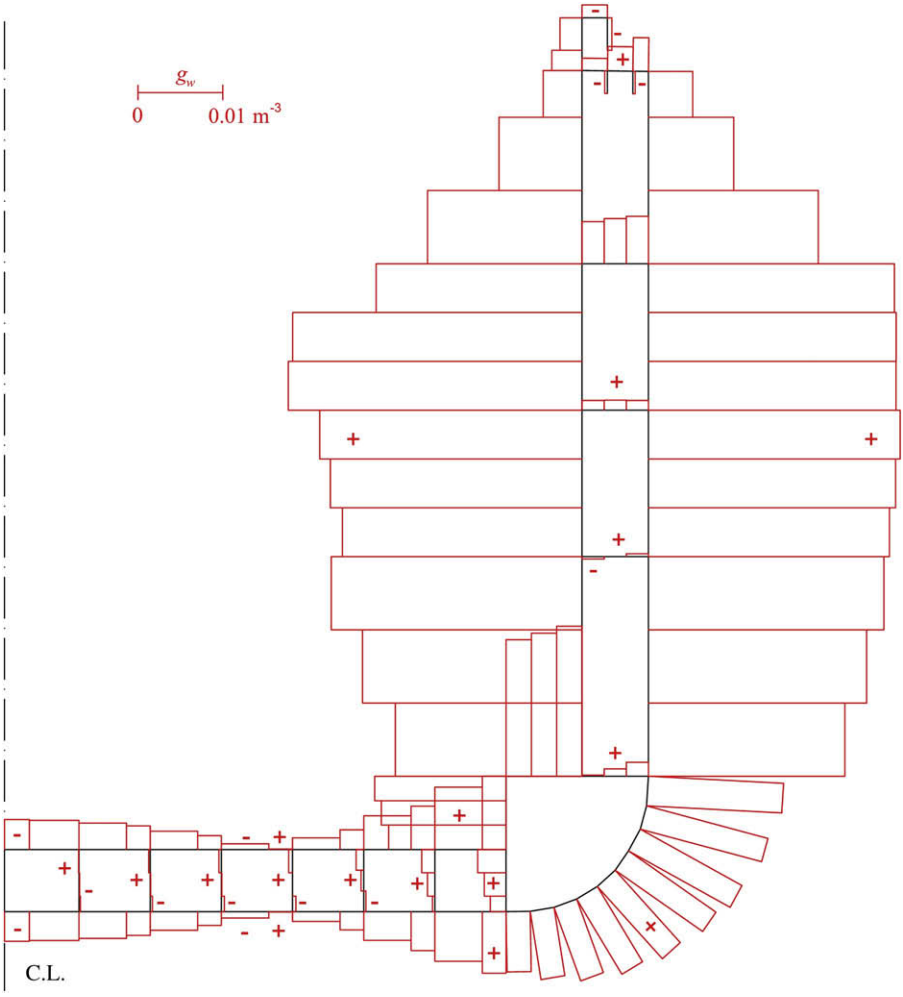

Fig. F4. Shear stress flow due to restrained warping.

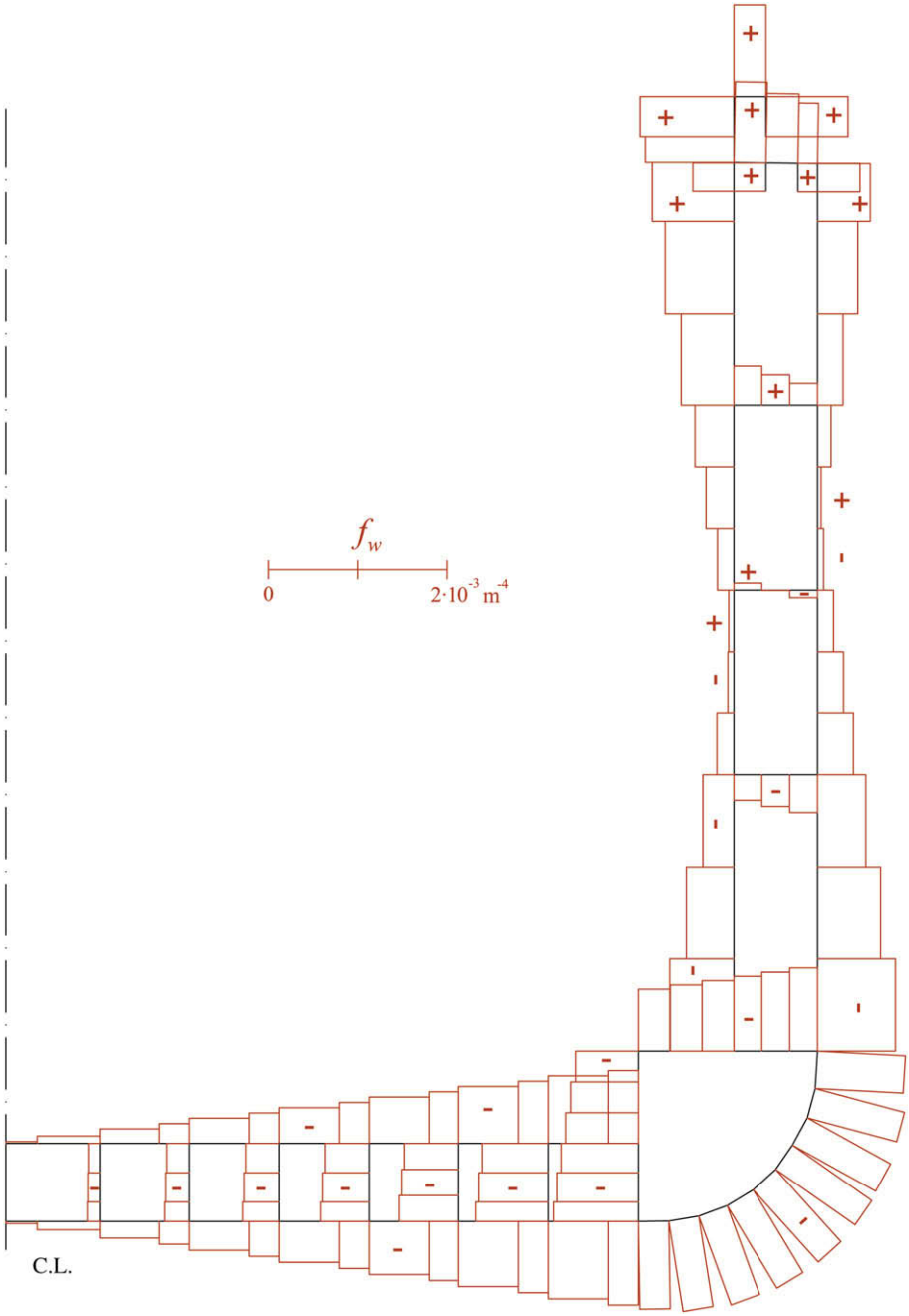

Fig. F5. Normal stress flow due to restrained warping.

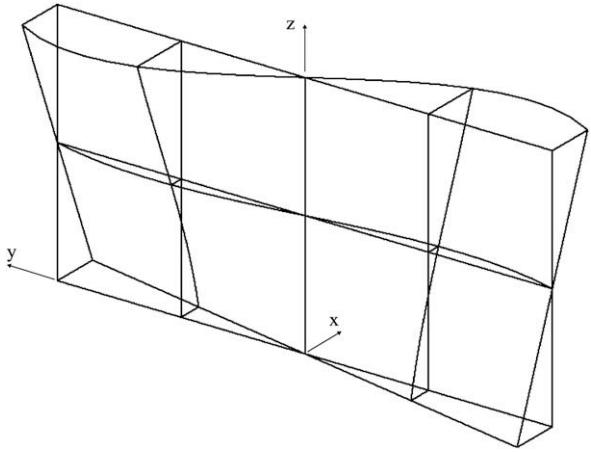

Fig. G1. Bulkhead deflection due to warping of cross-section.

$$\begin{bmatrix} \eta\, ch\, \eta l & \chi\, cos\, \chi l \\ \eta^3\, ch\, \eta l & -\chi^3\, cos\, \chi l \end{bmatrix} \begin{Bmatrix} A_1 \\ A_3 \end{Bmatrix} = \{0\}. \tag{A12}$$

For nontrivial solutions determinants of (A11) and (A12) have to be zero. That leads to the frequency equations

$$\eta\chi\left(\eta^2 + \chi^2\right) sh\, \eta l \sin \chi l = 0 \tag{A13}$$

$$\eta\chi\left(\eta^2 + \chi^2\right) ch\eta l \cos \chi l = 0 \tag{A14}$$

with the same eigenvalue formula for symmetric ($n = 0, 2\ldots$) and anti-symmetric ($n = 1, 3\ldots$) modes

$$\chi l = \frac{n\pi}{2}, \quad n = 0, 1, 2\ldots \tag{A15}$$

Substituting (A15) into (A7) for χ, one finds the following expression for natural frequencies of torsional vibrations

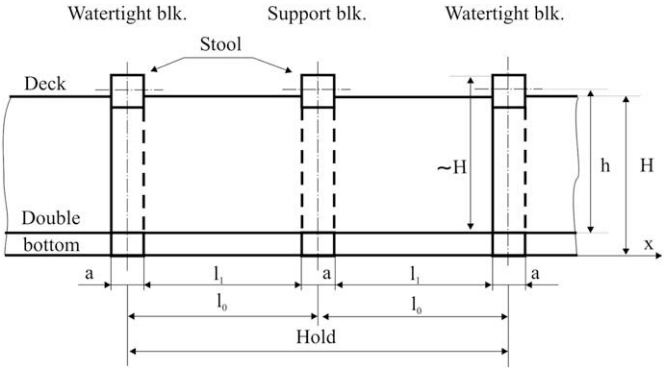

Fig. G2. Longitudinal section of container ship hold.

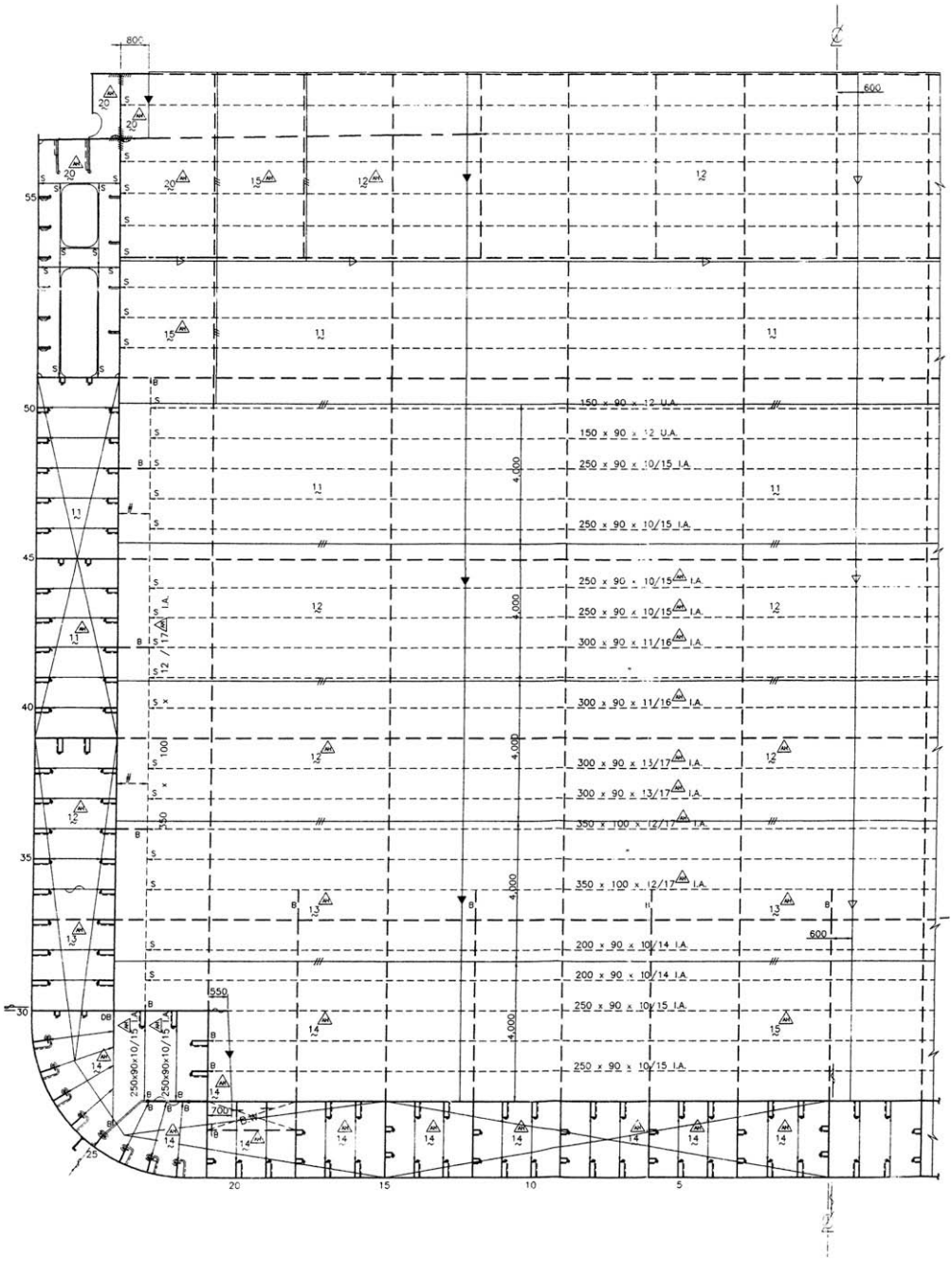

Fig. G3. Watertight bulkhead.

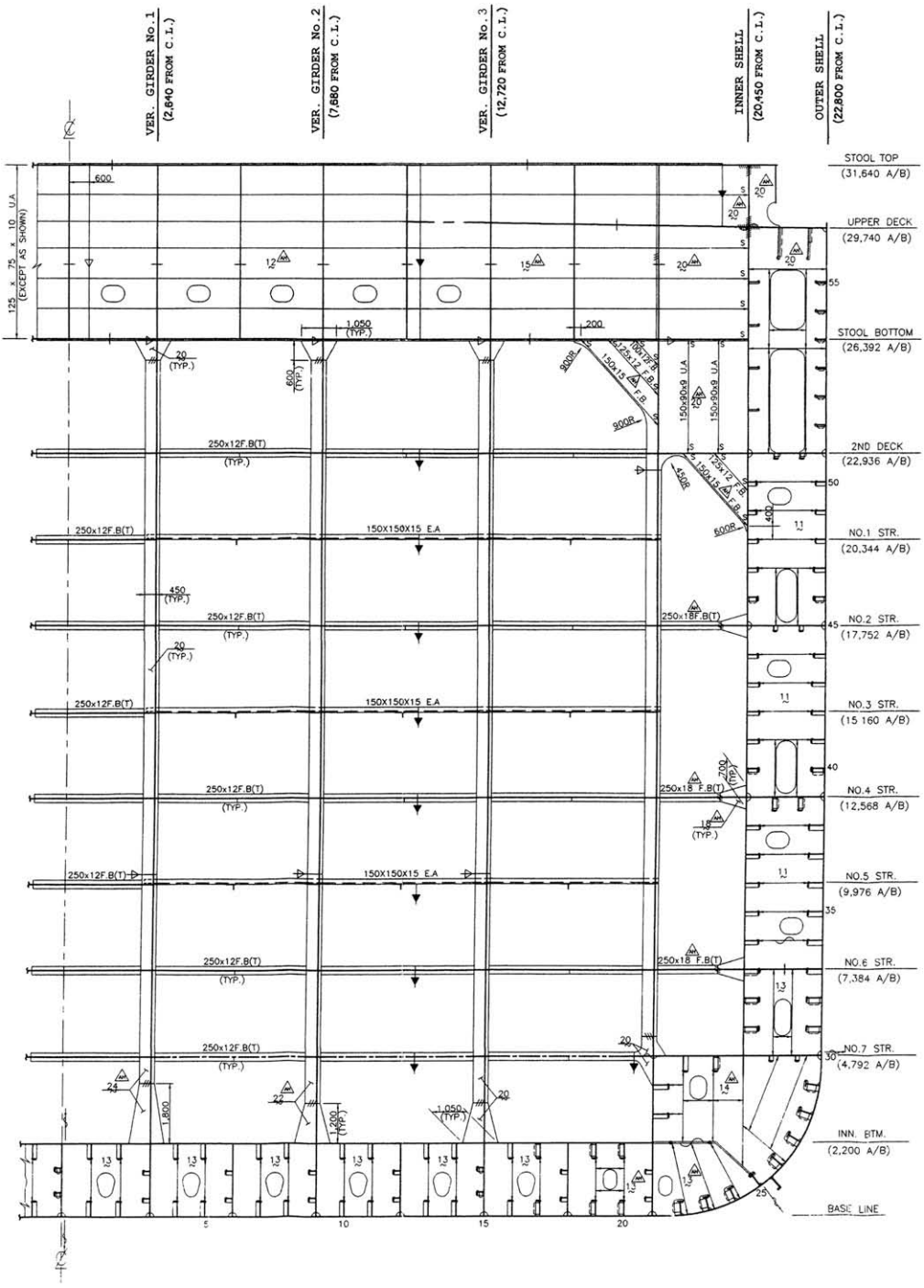

Fig. G4. Support bulkhead.

$$\omega_n = \frac{n\pi}{2l}\sqrt{\frac{GI_t}{J_t^0}}\frac{\sqrt{1+\left(\frac{n\pi}{2l}\right)^2\frac{EI_w}{GI_t}}}{\sqrt{1+\left(\frac{n\pi}{2l}\right)^2\frac{EI_w}{GI_s}}}, \quad n = 0, 1, 2\ldots \tag{A16}$$

The first term in the above formula represents natural frequencies of a free beam with free warping.

$$\tilde{\omega}_n = \frac{n\pi}{2l}\sqrt{\frac{GI_t}{J_t^0}}. \tag{A17}$$

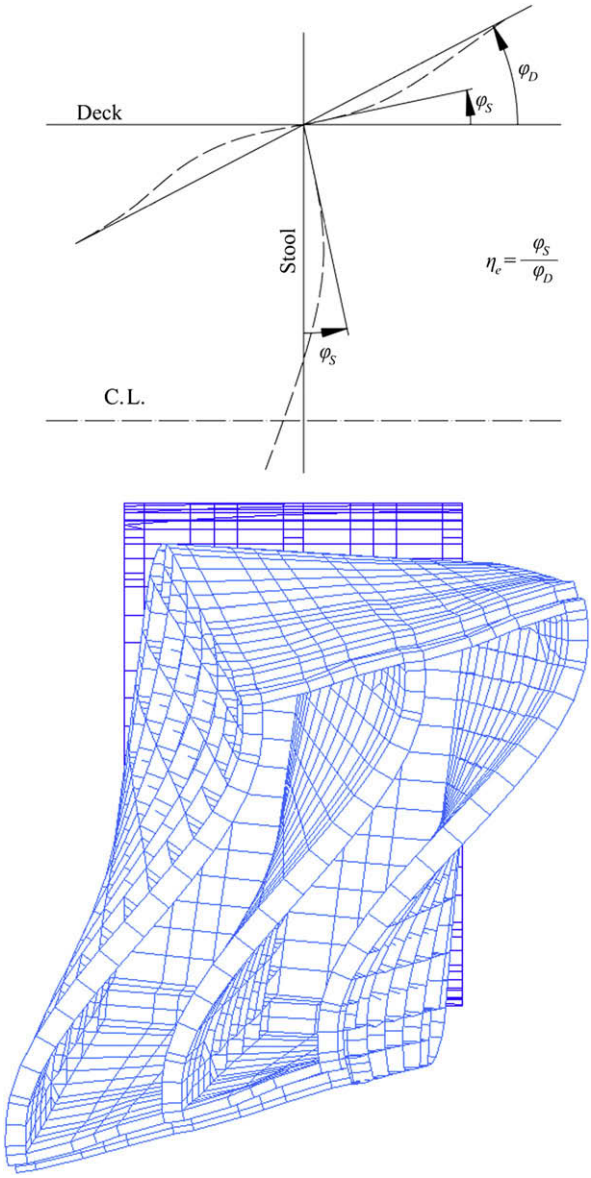

Fig. G5. Bird view on deformed bulkheads.

Warping stiffness EI_w in the nominator of (A16) increases natural frequencies as a result of restrained warping. Shear stiffness GI_s in the denominator reduces natural frequencies since additional twist angle due to shear influence acts as release.

Integration constants A_2 and A_4, and A_1 and A_3 are determined from (A11) and (A12), respectively. The symmetric and anti-symmetric modes according to (A8) yield

$$\psi_{tn} = \chi_n \sin \chi_n l \, ch \, \eta_n x + \eta_n \, sh \, \eta_n l \cos \chi_n x, \quad n = 0, 2\ldots \tag{A18}$$

$$\psi_{tn} = \chi_n \cos \chi_n l \, sh \, \eta_n x - \eta_n \, ch \, \eta_n l \sin \chi_n x, \quad n = 1, 3\ldots \tag{A19}$$

Referring to (23), the total twist angle consisted of torsion and shear contribution takes the following form

$$\psi_n = \left(1 - \frac{EI_w}{GI_s}\eta_n^2\right)\chi_n \sin \chi_n l \, ch \, \eta_n x + \left(1 + \frac{EI_w}{GI_s}\chi_n^2\right)\eta_n \, sh \, \eta_n l \cos \chi_n x, \quad n = 0, 2\ldots \tag{A20}$$

$$\psi_n = \left(1 - \frac{EI_w}{GI_s}\eta_n^2\right)\chi_n \cos \chi_n l \, sh \, \eta_n x - \left(1 - \frac{EI_w}{GI_s}\chi_n^2\right)\eta_n \, ch \, \eta_n l \sin \chi_n x, \quad n = 1, 3\ldots \tag{A21}$$

Appendix B. Consistent finite element properties, according to Eq. (37) (Frequency dependent formulation)

Bending-shear stiffness matrix:

$$[k]_{bs} = [k]_b + [k]_s \tag{B1}$$

$$k_{ij}^b = \frac{4EI_b}{l^3}\left[a_{i2}a_{j2} + \frac{3}{2}(a_{i2}a_{j3} + a_{i3}a_{j2}) + 3a_{i3}a_{j3}\right] \tag{B2}$$

$$k_{ij}^s = \frac{GA_s}{l}\left[b_{i1}b_{j1} + b_{i1}b_{j2} + b_{i2}b_{j1} + b_{i1}b_{j3} + b_{i3}b_{j1} + \frac{4}{3}b_{i2}b_{j2} + \frac{3}{2}(b_{i2}b_{j3} + b_{i3}b_{j2}) + \frac{9}{5}b_{i3}b_{j3}\right] \tag{B3}$$

The warping-shear stiffness matrix $[k]_{ws}$ is of the same constitution as $[k]_{bs}$, but I_b, A_s, a_{ik} and b_{ik} have to be replaced with I_w, I_s, d_{ik} and e_{ik}, respectively, Eqs. (35). Torsional stiffness matrix $[k]_t$ is of the same type as $[k]_s$, but A_s and b_{ik} have to be replaced with I_t and a_{ik}, respectively.

Shear-bending mass matrix

$$[m]_{sb} = [m]_s + [m]_b \tag{B4}$$

$$\begin{aligned} m_{ij}^s = ml\Bigg[& c_{i0}c_{j0} + \frac{1}{2}(c_{i1}c_{j0} + c_{i0}c_{j1}) + \frac{1}{3}(c_{i2}c_{j0} + c_{i1}c_{j1} + c_{i0}c_{j2}) \\ & + \frac{1}{4}(c_{i0}c_{j3} + c_{i1}c_{j2} + c_{i2}c_{j1} + c_{i3}c_{j0}) + \frac{1}{5}(c_{i1}c_{j3} + c_{i2}c_{j2} + c_{i3}c_{j1}) \\ & + \frac{1}{6}(c_{i2}c_{j3} + c_{i3}c_{j2}) + \frac{1}{7}c_{i3}c_{j3}\Bigg] \end{aligned} \tag{B5}$$

$$m_{ij}^b = \frac{J_b}{l}\left[a_{i1}a_{j1} + a_{i1}a_{j2} + a_{i2}a_{j1} + a_{i1}a_{j3} + a_{i3}a_{j1} + \frac{4}{3}a_{i2}a_{j2} + \frac{3}{2}(a_{i2}a_{j3} + a_{i3}a_{j2}) + \frac{9}{5}a_{i3}a_{j3}\right] \tag{B6}$$

The torsion-warping mass matrix $[m]_{tw}$ is of the same constitution as $[m]_{sb}$, but m, J_b, c_{ik}, and a_{ik} have to be replaced with J_t, J_w, f_{ik} and d_{ik} respectively, Eq. (35).

Shear-torsion mass matrix

$$\begin{aligned} m_{ij}^{st} = mcl\Big[& c_{i0}f_{j0} + \frac{1}{2}\Big(c_{i1}f_{j0} + c_{i0}f_{j1}\Big) + \frac{1}{3}\Big(c_{i2}f_{j0} + c_{i1}f_{j1} + c_{i0}f_{j2}\Big) \\ & + \frac{1}{4}\Big(c_{i0}f_{j3} + c_{i1}f_{j2} + c_{i2}f_{j1} + c_{i3}f_{j0}\Big) + \frac{1}{5}\Big(c_{i1}f_{j3} + c_{i2}f_{j2} + c_{i3}f_{j1}\Big) \\ & + \frac{1}{6}\Big(c_{i2}f_{j3} + c_{i3}f_{j2}\Big) + \frac{1}{7}c_{i3}f_{j3}\Big] \end{aligned} \tag{B7}$$

Shear load vector

$$q_i = q_0 l\left(c_{i0} + \frac{1}{2}c_{i1} + \frac{1}{3}c_{i2} + \frac{1}{4}c_{i3}\right) + q_1 l\left(\frac{1}{2}c_{i0} + \frac{1}{3}c_{i1} + \frac{1}{4}c_{i2} + \frac{1}{5}c_{i3}\right) \tag{B8}$$

Torsion load vector μ_i is of same form as (B8), expressed with μ_0, μ_1 and f_{ik}, Eqs. (35) and (39), instead of q_0, q_1 and e_{ik}, respectively. In all above formulae indeces i, j take values 1, 2, 3 and 4.

Appendix C. Consistent shape functions of finite element sectional forces

Bending moment, Eq. (2):

$$M_i = -EI_b \frac{\mathrm{d}^2 w_{bi}}{\mathrm{d}x^2} = -EI_b \left\langle a_{ik}^{(2)} \right\rangle \left\{ \xi^k \right\}, \quad k = 0, 1, 2, 3. \tag{C1}$$

Shear force, Eq. (3):

$$Q_i = GA_s \frac{\mathrm{d}w_{si}}{\mathrm{d}x} = GA_s \left\langle b_{ik}^{(1)} \right\rangle \left\{ \xi^k \right\}, \quad k = 0, 1, 2, 3. \tag{C2}$$

Pure torque, Eq. (7):

$$T_{ti} = GI_t \frac{\mathrm{d}\psi_{ti}}{\mathrm{d}x} = GI_t \left\langle d_{ik}^{(1)} \right\rangle \left\{ \xi^k \right\}, \quad k = 0, 1, 2, 3. \tag{C3}$$

Warping torque, Eq. (9):

$$T_{wi} = GI_s \frac{\mathrm{d}\psi_{si}}{\mathrm{d}x} = GI_s \left\langle e_{ik}^{(1)} \right\rangle \left\{ \xi^k \right\}, \quad k = 0, 1, 2, 3. \tag{C4}$$

Bimoment, Eq. (8):

$$B_{wi} = -EI_w \frac{\mathrm{d}^2 \psi_{ti}}{\mathrm{d}x^2} = -EI_w \left\langle d_{ik}^{(2)} \right\rangle \left\{ \xi^k \right\}, \quad k = 0, 1, 2, 3. \tag{C5}$$

Vectors of the shape functions, formulae (29) and (32):

$$\begin{aligned} \left\langle a_{ik}^{(2)} \right\rangle &= \tfrac{2}{l^2}\langle a_{i2}, 3a_{i3}, 0, 0\rangle \\ \left\langle b_{ik}^{(1)} \right\rangle &= \tfrac{1}{l}\langle b_{i1}, 2b_{i2}, 3b_{i3}, 0\rangle \\ \left\langle d_{ik}^{(1)} \right\rangle &= \tfrac{1}{l}\langle d_{i1}, 2d_{i2}, 3d_{i3}, 0\rangle \\ \left\langle e_{ik}^{(1)} \right\rangle &= \tfrac{1}{l}\langle e_{i1}, 2e_{i2}, 3e_{i3}, 0\rangle \\ \left\langle d_{ik}^{(2)} \right\rangle &= \tfrac{2}{l^2}\langle d_{i2}, 3d_{i3}, 0, 0\rangle \end{aligned} \tag{C6}$$

Appendix D. Simplified finite element properties, from Appendix B (Frequency independent formulation)

Stiffness matrices:

$$[k]_{bs} = \frac{2EI_b}{(1+12\beta)l^3}\begin{bmatrix} 6 & 3l & -6 & 3l \\ & 2(1+3\beta)l^2 & -3l & (1-6\beta)l^2 \\ & & 6 & -3l \\ Sym. & & & 2(1+3\beta)l^2 \end{bmatrix} \tag{D1}$$

$$[k]_{ws} = \frac{2EI_w}{(1+12\gamma)l^3}\begin{bmatrix} 6 & 3l & -6 & 3l \\ & 2(1+3\gamma)l^2 & -3l & (1-6\gamma)l^2 \\ & & 6 & -3l \\ Sym. & & & 2(1+3\gamma)l^2 \end{bmatrix} \tag{D2}$$

$$[k]_t = \frac{GI_t}{30(1+12\gamma)^2 l}\begin{bmatrix} 36 & 3(1-60\gamma)l & -36 & 3(1-60\gamma)l \\ & 4(1+15\gamma+360\gamma^2)l^2 & -3(1-60\gamma)l & -(1+60\gamma-720\gamma^2)l^2 \\ & & 36 & -3(1-60\gamma)l \\ Sym. & & & 4(1+15\gamma+360\gamma^2)l^2 \end{bmatrix} \tag{D3}$$

Mass matrices:

$$[m]_{sb} = [m]_s + [m]_b \tag{D4}$$

$$[m]_s = \frac{ml}{420(1+12\beta)^2} \times \begin{bmatrix} 156+3528\beta+20160\beta^2 & \left(22+462\beta+2520\beta^2\right)l & 54+1512\beta+10080\beta^2 & -\left(13+378\beta+2520\beta^2\right)l \\ & \left(4+84\beta+504\beta^2\right)l^2 & \left(13+378\beta+2520\beta^2\right)l & -\left(3+84\beta+504\beta^2\right)l^2 \\ & & 156+3528\beta+20160\beta^2 & -\left(22+462\beta+2520\beta^2\right)l \\ Sym. & & & \left(4+84\beta+504\beta^2\right)l^2 \end{bmatrix} \tag{D5}$$

$$[m]_b = \frac{J_b}{30(1+12\beta)^2 l}\begin{bmatrix} 36 & (3-180\beta)l & -36 & (3-180\beta)l \\ & \left(4+60\beta+1440\beta^2\right)l^2 & (-3+180\beta)l & -\left(1+60\beta-720\beta^2\right)l^2 \\ & & 36 & (-3+180\beta)l \\ Sym. & & & \left(4+60\beta+1440\beta^2\right)l^2 \end{bmatrix} \tag{D6}$$

$$[m]_{tw} = [m]_t + [m]_w \tag{D7}$$

$$[m]_t = \frac{J_t l}{420(1+12\gamma)^2} \times \begin{bmatrix} 156+3528\gamma+20160\gamma^2 & (22+462\gamma+2520\gamma^2)l & 54+1512\gamma+10080\gamma^2 & -(13+378\gamma+2520\gamma^2)l \\ & (4+84\gamma+504\gamma^2)l^2 & (13+378\gamma+2520\gamma^2)l & -(3+84\gamma+504\gamma^2)l^2 \\ & & 156+3528\gamma+20160\gamma^2 & -(22+462\gamma+2520\gamma^2)l \\ Sym. & & & (4+84\gamma+504\gamma^2)l^2 \end{bmatrix} \tag{D8}$$

$$[m]_w = \frac{J_w}{30(1+12\gamma)^2 l}\begin{bmatrix} 36 & (3-180\gamma)l & -36 & (3-180\gamma)l \\ & (4+60\gamma+1440\gamma^2)l^2 & (-3+180\gamma)l & -(1+60\gamma-720\gamma^2)l^2 \\ & & 36 & (-3+180\gamma)l \\ Sym. & & & (4+60\gamma+1440\gamma^2)l^2 \end{bmatrix} \tag{D9}$$

$$[m]_{st} = \frac{mlc}{420(1+12\beta)(1+12\gamma)} \times \begin{bmatrix} 156+1764\beta+1764\gamma+20160\beta\gamma & (22+252\beta+210\gamma+2520\beta\gamma)l & 54+756\beta+756\gamma+10080\beta\gamma & -(13+168\beta+210\gamma+2520\beta\gamma)l \\ (22+210\beta+252\gamma+2520\beta\gamma)l & (4+42\beta+42\gamma+504\beta\gamma)l^2 & (13+210\beta+168\gamma+2520\beta\gamma)l & -(3+42\beta+42\gamma+504\beta\gamma)l^2 \\ 54+756\beta+756\gamma+10080\beta\gamma & (13+168\beta+210\gamma+2520\beta\gamma)l & 156+1764\beta+1764\gamma+20160\beta\gamma & -(22+252\beta+210\gamma+2520\beta\gamma)l \\ -(13+210\beta+168\gamma+2520\beta\gamma)l & -(3+42\beta+42\gamma+504\beta\gamma)l^2 & -(22+210\beta+252\gamma+2520\beta\gamma)l & (4+42\beta+42\gamma+504\beta\gamma)l^2 \end{bmatrix} \tag{D10}$$

$$[m]_{ts} = [m]_{st}^T \tag{D11}$$

Load vectors:

$$\{q\} = \frac{q_0 l}{12}\begin{Bmatrix} 6 \\ l \\ 6 \\ -l \end{Bmatrix} + \frac{q_1 l}{60(1+12\beta)}\begin{Bmatrix} 9+120\beta \\ (2+30\beta)l \\ 21+240\beta \\ -(3+30\beta)l \end{Bmatrix} \tag{D12}$$

$$\{\mu\} = \frac{\mu_0 l}{12}\begin{Bmatrix} 6 \\ l \\ 6 \\ -l \end{Bmatrix} + \frac{\mu_1 l}{60(1+12\gamma)}\begin{Bmatrix} 9+120\gamma \\ (2+30\gamma)l \\ 21+240\gamma \\ -(3+30\gamma)l \end{Bmatrix} \tag{D13}$$

Stiffness ratios:

$$\beta = \frac{EI_b}{GA_s l^2}, \quad \gamma = \frac{EI_w}{GI_s l^2}. \tag{D14}$$

Appendix E. Estimation of inaccuracy due to application of inconsistent finite element formulation

The beam finite element properties are determined by the energy approach, employing both the frequency dependent and independent shape functions. The former formulation is based on the consistent vibration beam theory, while the latter follows the static beam theory. Accuracy of the simplified formulation can be evaluated analysing natural vibrations of prismatic beam by the energy method. The governing equation for flexural natural frequencies is deduced from the energy balance, Eq. (26), in the form of Rayleigh quotient

$$\omega^2 = \frac{EI\int_0^L \left(\frac{d^2 w_b}{dx^2}\right)^2 dx + GA_s \int_0^L \left(\frac{dw_s}{dx}\right)^2 dx}{m\int_0^L w^2 dx + J\int_0^L \left(\frac{dw_b}{dx}\right)^2 dx}. \tag{E1}$$

For the reason of simplicity let us use the sinusoidal natural modes into account

$$w_{bn} = \sin\frac{n\pi x}{L}. \tag{E2}$$

In that case the shear and total deflection according to (24) read

$$w_{sn} = \left[-\omega^2\frac{J}{GA_s} + \left(\frac{n\pi}{L}\right)^2\frac{EI}{GA_s}\right]\sin\frac{n\pi x}{L} \tag{E3}$$

$$w_n = \left[1 - \omega^2\frac{J}{GA_s} + \left(\frac{n\pi}{L}\right)^2\frac{EI}{GA_s}\right]\sin\frac{n\pi x}{L}. \tag{E4}$$

By substituting (E2)–(E4) into (E1), and taking into account

$$\int_0^L \sin^2\frac{n\pi x}{L}dx = \int_0^L \cos^2\frac{n\pi x}{L}dx = \frac{L}{2} \tag{E5}$$

yields

$$\omega^2 = \left(\frac{n\pi}{L}\right)^2\frac{EI}{m}\frac{\left(\frac{n\pi}{L}\right)^2 + \frac{GA_s}{EI}\left[\left(\frac{n\pi}{L}\right)^2\frac{EI}{GA_s} - \omega_n^2\frac{J}{GA_s}\right]^2}{\left[1 + \left(\frac{n\pi}{L}\right)^2\frac{EI}{GA_s} - \omega_n^2\frac{J}{GA_s}\right]^2 + \left(\frac{n\pi}{L}\right)^2\frac{J}{m}}. \tag{E6}$$

Since both the modal stiffness (nominator) and modal mass (denominator) depend on the unknown natural frequency ω_n (as in the finite element formulation), an iteration procedure has to be used to solve the implicit Eq. (E6). The convergence is very fast due to small influence of ω_n^2 on the right hand side of (E6).

However, Eq. (E6) can also be solved in a close form if it is written as a polynomial. It is obvious that we are faced with the polynomial of 3rd order per ω_n^2, which can be written as product of two polynomials

$$P_3\left(\omega_n^2\right) = P_1\left(\omega_n^2\right)P_2\left(\omega_n^2\right) = 0, \tag{E7}$$

where

Table E1
Natural frequencies of prismatic pontoon, ω_i (Hz).

Mode no.	Exact (E8), *a*	Approximate (E9), *b*	$J=0$ (E10), *c*	Discrepancy %	
				$b/a-1$	$c/a-1$
1	0.7540	0.7541	0.7588	0.00	0.63
2	2.1418	2.1422	2.1560	0.02	0.65
3	3.5739	3.5745	3.5900	0.02	0.45
4	4.9789	4.9796	4.9940	0.01	0.30
5	6.3610	6.3617	6.3745	0.01	0.21
6	7.7278	7.7284	7.7397	0.01	0.15
7	9.0844	9.0850	9.0951	0.01	0.12
8	10.4342	10.4347	10.4437	0.01	0.09
9	11.7791	11.7796	11.7877	0.00	0.07
10	13.1205	13.1209	13.1284	0.00	0.06

$$P_1\left(\omega_n^2\right) = \frac{J}{GA_s}\omega_n^2 - \left[1+\left(\frac{n\pi}{L}\right)^2\frac{EI}{GA_s}\right] \tag{E8}$$

$$P_2\left(\omega_n^2\right) = \frac{J}{GA_s}\omega_n^4 - \left[1+\left(\frac{n\pi}{L}\right)^2\left(\frac{EI}{GA_s}+\frac{J}{m}\right)\right]\omega_n^2 + \left(\frac{n\pi}{L}\right)^4\frac{EI}{m}. \tag{E9}$$

The solution of $P_1(\omega_n^2) = 0$ doesn't have physical meaning, as well as the first eigenvalue of $P_2(\omega_n^2) = 0$. Its second eigenvalue represents the actual natural frequencies

$$\omega_n^2 = \frac{GA_s}{2J}\left\{\left[1+\left(\frac{n\pi}{L}\right)^2\left(\frac{EI}{GA_s}+\frac{J}{m}\right)\right] - \left\{\left[1+\left(\frac{n\pi}{L}\right)^2\left(\frac{EI}{GA_s}+\frac{J}{m}\right)\right]^2 - 4\left(\frac{n\pi}{L}\right)^4\frac{EI}{GA_s}\frac{J}{m}\right\}^{\frac{1}{2}}\right\}. \tag{E10}$$

It is interesting to point out that polynomial $P_2(\omega_n^2)$ is identical to the frequency equation of the uncoupled flexural vibrations, which yields from Eq. (20).

In case of static displacement relations, Eqs. (E3) and (E4) with $\omega = 0$, Eq. (E6) is reduced to the approximate formula for determining natural frequencies

$$\omega_n^2 = \left(\frac{n\pi}{L}\right)^4\frac{EI}{m}\frac{1+\left(\frac{n\pi}{L}\right)^2\frac{EI}{GA_s}}{\left[1+\left(\frac{n\pi}{L}\right)^2\frac{EI}{GA_s}\right]^2+\left(\frac{n\pi}{L}\right)^2\frac{J}{m}}. \tag{E11}$$

Furthermore, if mass rotation is neglected, i.e. $J = 0$, one finds from (E11)

$$\omega_n^2 = \frac{\left(\frac{n\pi}{L}\right)^4\frac{EI}{m}}{1+\left(\frac{n\pi}{L}\right)^2\frac{EI}{GA_s}}. \tag{E12}$$

In order to estimate reliability of the approximate solution (E11) and influence of mass rotation on natural frequencies, Eq. (E12), let us analyse vibrations of a pontoon with the cross-section parameters of a real ship specified in Section 6: $L = 348$ m, $A = 7.049$ m^2, $A_{sy} = 1.056$ m^2, $I_{bz} = 2428$ m^4, $m = 100$ t/m, $E = 2.1\cdot 10^8$ kN/m^2, $\nu = 0.3$, $E/G = 2(1+\nu)$, $(J/m) = (I_{bz}/A)$. The calculated values of natural frequencies in the above considered cases are listed in Table E1.

Discrepancies between the approximate and the exact solution are very small and negligible. The solution for $J = 0$ shows some differences at the first modes, but for the higher modes it converges to the exact solution.

Appendix F. Ship cross-section properties

Geometrical properties of a thin-walled girder include cross-section area A, moment of inertia of cross-section I_b, shear area A_s, torsional modulus I_t, warping modulus I_w and shear inertia modulus I_s. These parameters are determined analytically for a simple cross-section as pure geometrical properties [12,13,17,18].

However, determination of cross-section properties for an open multi-cell cross-section, as in case of ship structures, is quite a difficult task. Therefore, the strip element method is applied for solving this statically indetermined problem [29]. Firstly, axial node displacements are calculated due to bending caused by shear force, and due to torsion caused by variation of twist angle. Then, shear stress in bending τ_b, shear stress due to pure torsion τ_t, shear and normal stresses due to restrained warping τ_w and σ_w, respectively, are determined. Based on the equivalence of strain energies induced by sectional forces and calculated stresses, it is possible to specify cross-section properties in the same formulation as presented below. Furthermore, those formulae can be expressed by stress flows, i.e. stresses due to unit sectional forces [14,25].

Shear area:

$$A_s = \frac{Q^2}{\int_A \tau_b^2 \mathrm{d}A} = \frac{1}{\int_A g_b^2 \mathrm{d}A}, \quad g_b = \frac{\tau_b}{Q}. \tag{F1}$$

Torsional modulus:

$$I_t = \frac{T_t^2}{\int_A \tau_t^2 \mathrm{d}A} = \frac{1}{\int_A g_t^2 \mathrm{d}A}, \quad g_t = \frac{\tau_t}{T_t}. \tag{F2}$$

Shear inertia modulus:

$$I_s = \frac{T_w^2}{\int_A \tau_w^2 \mathrm{d}A} = \frac{1}{\int_A g_w^2 \mathrm{d}A}, \quad g_w = \frac{\tau_w}{T_w}. \tag{F3}$$

Warping modulus:

$$I_w = \frac{B_w^2}{\int_A \sigma_w^2 \mathrm{d}A} = \frac{1}{\int_A f_w^2 \mathrm{d}A}, \quad f_w = \frac{\sigma_w}{B_w}. \tag{F4}$$

The above quantities are not pure geometrical cross-section properties any more, since they also depend on Poisson's ratio as a physical parameter.

For a ship in lightweight loading condition the mass parameters can be determined approximately based on the given mass distribution per unit length, m, and calculated cross-section parameters, i.e.

$$J_b = \frac{m}{A} I_b, \; J_t^0 = \frac{m}{A}\left(I_{by} + I_{bz}\right), \; J_w = \frac{m}{A} I_w \tag{F5}$$

Stress flows at midship section for the considered ship, determined by program STIFF [24], are shown in Figs. F1–F5. The midship section properties are the following:

Cross-section area, $A = 7.049\ \mathrm{m}^2$
Vertical shear area, $A_{sz} = 1.604\ \mathrm{m}^2$
Horizontal shear area, $A_{sy} = 1.056\ \mathrm{m}^2$
Vertical position of centroid, $z_C = 13.36$ m
Vertical position of shear centre, $z_S = -15.61$ m
Vertical moment of inertia, $I_{by} = 1040\ \mathrm{m}^4$
Horizontal moment of inertia, $I_{bz} = 2428\ \mathrm{m}^4$

Torsional modulus, $I_t = 20.20\ \mathrm{m}^4$
Shear inertia modulus, $I_s = 927\ \mathrm{m}^4$
Warping modulus, $I_w = 321500\ \mathrm{m}^6$.

Appendix G. Contribution of transverse bulkheads to hull stiffness

This problem for container ships is extensively analysed in [31], where torsional modulus of ship cross-section is increased proportionally to the bulkhead strain energy. The bulkhead is considered as an orthotropic plate with very strong stool [32]. The bulkhead strain energy is determined for the given warping of cross-section as a boundary condition. The warping causes bulkhead screwing and bending. Here, only the review of the final results is presented.

The bulkhead deflection (axial displacement) is given by the following formula, Fig. G1:

$$u(y,z) = -y\left\{\left(z-d\right) + \left[1-\left(\frac{y}{b}\right)^2\right]\frac{z^2}{H}\left(2-\frac{z}{H}\right)\right\}\psi', \tag{G1}$$

where H is the ship height, b is one half of bulkhead breadth, d is the distance of warping centre from double bottom neutral line, y and z are transverse and vertical coordinates, respectively, and ψ' is the variation of twist angle.

The bulkhead grillage strain energy includes vertical and horizontal bending with contraction, and torsion [30].

$$U_g = \frac{1}{1-\nu^2}\left[\frac{116H^3}{35b}i_y + \frac{32b^3}{105H}i_z + \frac{8Hb}{75}\nu(i_y+i_z) + \frac{143Hb}{75}(1-\nu)i_t\right]E\psi'^2, \tag{G2}$$

where i_y, i_z and i_t are the average moments of inertia of cross-section and torsional modulus per unit breadth, respectively.

The stool strain energy is comprised of the bending, shear and torsional contributions

$$U_s = \left[\frac{12h^2 I_{sb}}{b} + 72(1+\nu)\frac{h^2}{b^3}\frac{I_{sb}^2}{A_s} + \frac{9bI_{st}}{10(1+\nu)}\right]E\psi'^2, \tag{G3}$$

where I_{sb}, A_s and I_{st} are the moment of inertia of cross-section, shear area and torsional modulus, respectively. Quantity h is the stool distance from the inner bottom, Fig. G2.

The equivalent torsional modulus yields, Fig. G2

$$I_t^* = \left[1 + \frac{a}{l_1} + \eta_e\frac{4(1+\nu)C}{I_t l_0}\right]I_t, \tag{G4}$$

Table G1
Stiffness parameters of watertight bulkhead.

Girder	Moment of inertia, I [m^4]	Torsional modulus, I_t [m^4]	Girder spacing, c [m]	Moment of inertia per unit breadth, i [m^3]	Torsional modulus per unit breadth, i_t [m^3]
Horizontal	0.02160	0.00905	5.184	0.004164	0.002843
Vertical	0.03094	0.02333	5.04	0.006139	

Table G2
Stiffness parameters of support bulkhead.

Girder	Moment of inertia, I [m^4]	Torsional modulus, I_t [m^4]	Girder spacing, c [m]	Moment of inertia per unit breadth, i [m^3]	Torsional modulus per unit breadth, i_t [m^3]
Horizontal	0.00972	0.00486	5.184	0.001875	0.002293
Vertical	0.02017	0.02827	5.04	0.004002	

Table G3
Stool stiffness parameters.

Shear area	Moment of inertia	Torsional modulus
A_s [m^2]	I_s [m^4]	I_{ts} [m^4]
0.045	0.12236	0.433

Table G4
Bulkhead strain energy, $U/[E\psi'^2]$

Measure	Watertight bulkhead		Support bulkhead		Energy coefficient
	Grillage	Stool	Grillage	Stool	C, Eq. (D5)
(1)	(2)	(3)	(4)	(5)	(6) = [(2)+(3)+(4)+(5)]/2
$U/[E\psi'^2]$	22.856	69.708	11.341	69.708	86.807

where a is the web height of bulkhead girders (frame spacing), l_0 is the bulkhead spacing, $l_1 = l_0 - a$ is the net length, η_e is the efficiency factor, and C is the energy coefficient

$$C = \frac{U_g + U_s}{E\psi'^2}. \tag{G5}$$

The second term in (G4) is the main contribution of the bulkhead as the closed cross-section segment of ship hull, and the third one comprises the bulkhead strain energy.

Large container ships are designed with alternate watertight and support bulkheads, Fig. G2. These bulkheads for the considered ship are shown in Figs. G3 and G4. The stiffness parameters of the bulkhead girders are listed in Tables G1 and G2, while the stool parameters are given in Table G3. The bulkhead dimensions are the following:

$$H = 29.74\,m, \quad b = 20.45\,m, \quad l_0 = 14.44\,m, \quad a = 1.81\,m.$$

The bulkhead strain energy, determined according to (G2) and (G3), is summarized in Table G4, where also the energy coefficient is calculated as the average value of the watertight and support bulkhead strain energies. Most of the hull induced energy is absorbed by the stool. The efficiency factor, η_e, takes into account the release of the bulkhead support, Fig. G5. It can be expressed as the ratio of the stool boundary rotation angle and the global deck rotation angle. In the considered case, $\eta_e = 0.55$. Thus, the equivalent torsional modulus for midship section yields $I_t^* = 1.9 I_t$. This value is applied for all ship cross-sections as the first approximation.

Appendix H. Formulation of effective stiffness of thin-walled girders

It is well known that Timoshenko's beam theory for flexural vibrations with the shear area included is valid for the first couple natural modes. In literature there is a large number of references dealing

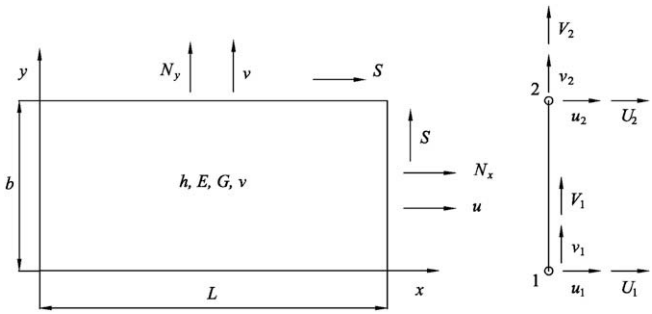

Fig. H1. Membrane strip element.

with effective stiffness parameters in order to increase validity of beam model to higher modes as for instance [33–37]. One way is to keep moment of inertia of cross-section constant and to vary shear area, and another is to vary both parameters, [38]. Since shear deflection is increasing and pure bending deflection is decreasing for higher modes, the former treatment is artificial one, while the latter is physically consistent and therefore preferable.

Energy approach for determining effective stiffness of thin-walled girders for flexural and torsional vibrations is described in details in [14]. Here, only the basic idea and main formulae for flexural vibrations are presented informatively.

One half of ship cross-section is divided into strip elements stretching in axial direction, which can be of the following types: membrane, plate, bar and beam. In order to avoid the distortion of cross-section, all transverse bulkheads within assumed prismatic hull are condensed in one bulkhead of common thickness and modelled by ordinary membrane finite elements.

A membrane strip element, with geometric and physical characteristics, nodal forces and displacements, is shown in Fig. H1. Displacement field is described by harmonic functions, that is valid for simply supported edges

$$\{f\} = \begin{Bmatrix} u \\ v \end{Bmatrix} = [\phi]\{\delta\}, \tag{H1}$$

where

$$\begin{aligned} &[\phi] = [\phi]_C \cos\alpha_n x + [\phi]_S \sin\alpha_n x, \quad \alpha_n = \tfrac{n\pi}{L}, \quad n = 1, 2\ldots \\ &[\phi]_C = \begin{bmatrix} \phi_1 & 0 & \phi_2 & 0 \\ 0 & 0 & 0 & 0 \end{bmatrix}, \quad [\phi]_S = \begin{bmatrix} 0 & 0 & 0 & 0 \\ 0 & \phi_1 & 0 & \phi_2 \end{bmatrix} \\ &\{\delta\} = \begin{Bmatrix} u_1 \\ v_1 \\ u_2 \\ v_2 \end{Bmatrix}. \end{aligned} \tag{H2}$$

Functions ϕ_1 and ϕ_2 are the linear strip shape functions

$$\phi_1 = 1 - \eta, \quad \phi_2 = \eta, \quad \eta = y/b. \tag{H3}$$

Furthermore, membrane deformation field reads

$$\{\epsilon\} = [L]\{\delta\} = [\Lambda][\phi]\{\delta\}, \tag{H4}$$

where $[\Lambda]$ is the membrane differential operator

$$[\Lambda] = \begin{bmatrix} \dfrac{\partial}{\partial x} & 0 \\ 0 & \dfrac{\partial}{\partial y} \\ \dfrac{\partial}{\partial y} & \dfrac{\partial}{\partial x} \end{bmatrix} \tag{H5}$$

leading to

$$\begin{aligned} &[L] = [L]_C \cos\alpha_n x + [L]_S \sin\alpha_n x \\ &[L]_C = \begin{bmatrix} 0 & 0 & 0 & 0 \\ 0 & 0 & 0 & 0 \\ \phi_1' & \alpha_n\phi_1 & \phi_2' & \alpha_n\phi_2 \end{bmatrix}, \quad [L]_S = \begin{bmatrix} -\alpha_n\phi_1 & 0 & -\alpha_n\phi_2 & 0 \\ 0 & \phi_1' & 0 & \phi_2' \\ 0 & 0 & 0 & 0 \end{bmatrix}. \end{aligned} \tag{H6}$$

The membrane elasticity matrix reads

$$[D] = \frac{h}{1-\nu^2}\begin{bmatrix} E & \nu E & 0 \\ \nu E & E & 0 \\ 0 & 0 & (1-\nu^2)G \end{bmatrix}. \tag{H7}$$

According to the definition of stiffness matrix in the finite element method, and by employing (H3), one finds separated normal and shear stiffness matrices

$$[K] = \int_0^L \int_0^b [L]^T[D][L]\mathrm{d}x\mathrm{d}y = [K]_E + [K]_G, \tag{H8}$$

where

$$[K]_E = \frac{ELh}{2(1-\nu^2)b}\begin{bmatrix} \frac{\beta_n^2}{3} & \frac{\nu\beta_n}{2} & \frac{\beta_n^2}{6} & -\frac{\nu\beta_n}{2} \\ & 1 & \frac{\nu\beta_n}{2} & -1 \\ & & \frac{\beta_n^2}{3} & -\frac{\nu\beta_n}{2} \\ Sym. & & & 1 \end{bmatrix}$$

$$[K]_G = \frac{GLh}{2b}\begin{bmatrix} 1 & -\frac{\beta_n}{2} & -1 & -\frac{\beta_n}{2} \\ & \frac{\beta_n^2}{3} & \frac{\beta_n}{2} & \frac{\beta_n^2}{6} \\ & & 1 & \frac{\beta_n}{2} \\ Sym. & & & \frac{\beta_n^2}{3} \end{bmatrix} \tag{H9}$$

$$\beta_n = \alpha_n b = \frac{n\pi b}{L}.$$

By following the standard finite element procedure for assembling of finite elements, the system equation for each the nth mode yields

$$([K]_{En} + [K]_{Gn})\{\delta\}_n = \frac{L}{2}\{q\}_n, \tag{H10}$$

where q_n is the amplitude of the assumed vertical and horizontal load for vertical and horizontal bending, respectively.

Shear force Q and bending moment M are obtained by single and double integration of harmonic load q along prismatic hull, respectively. Thus, their amplitudes for complete cross-section read

$$Q_n = \frac{2}{\alpha_n}\sum_{i=1}^{k} q_n^i, \quad M_n = \frac{2}{\alpha_n^2}\sum_{i=1}^{k} q_n^i, \tag{H11}$$

where k is number of loaded nodes at one half of cross-section.

Table H1
The 5th natural frequencies with effective stiffness, ω_5 (Hz).

Vibration type	1D FEM		3D FEM	Discrepancy %	
	$a_5^* = 0.804$	$a_5^* = 0.3$		$a_5^* = 0.804$	$a_5^* = 0.3$
Horizontal	6.864	4.665	6.798	0.97	−31.38
Coupled	3.029	2.687	2.630	15.17	2.17

Furthermore, the bending and shear strain energy for the uniform hull due to harmonic M and Q take values

$$\begin{aligned} U_{Mn} &= \frac{1}{2EI_n}\int_0^L M^2 \mathrm{d}x = \frac{LM_n^2}{4EI_n} \\ U_{Qn} &= \frac{1}{2GA_{Sn}}\int_0^L Q^2 \mathrm{d}x = \frac{LQ_n^2}{4GA_{Sn}}. \end{aligned} \tag{H12}$$

On the other side, the bending and shear strain energy for complete hull are also obtained by multiplying Eq. (H10) with $\langle\delta\rangle_n$. Finally, equalizing those expressions with (H12), one finds formulae for effective moment of inertia of cross-section and shear area, respectively

$$\begin{aligned} I_n &= \frac{LM_n^2}{4E\langle\delta\rangle_n[K]_{En}\{\delta\}_n} \\ A_{Sn} &= \frac{LQ_n^2}{4G\langle\delta\rangle_n[K]_{Gn}\{\delta\}_n}. \end{aligned} \tag{H13}$$

The effective coefficients are $i_n = I_n/I_0$ and $a_n = A_{Sn}/A_{S0}$. In similar way, the torsional effective stiffness parameters can also be determined, [14].

If one prefers to keep the value of moment of inertia of cross-section constant and to vary shear area only, than complete strain energy has to be used for shear area correction. By employing the following relation yielding from Eqs. (H11)

$$M_n = \frac{Q_n}{\alpha_n}, \tag{H14}$$

and after some manipulations one finds

$$a_n^* = \frac{a_n}{1 + \dfrac{1}{2(1+\nu)\alpha_n^2}\dfrac{A_s}{I}\dfrac{a_n}{i_n}}. \tag{H15}$$

In the considered numerical example, the horizontal stiffness parameters for midship section read: $A_{sy} = 1.056\ \mathrm{m}^2$, $I_{bz} = 2428\ \mathrm{m}^4$, Appendix F. This leads to $a_5^* = 0.804$ and the modified natural frequencies are listed in Table G1. Discrepancy between 1D and 3D natural frequencies is considerably reduced in the case of horizontal vibrations, while that of the coupled vibrations is still high. By taking $a_5^* = 0.3$ into account, the effect is opposite, Table H1. It is obvious that unrealistic ratio of the bending and shear deflection, combined with torsional properties in coupled vibrations results with incorrect frequency values. So, the conclusion is that effective values of both bending and shear stiffnesses have to be taken into account in order to simultaneously minimize the discrepancies of flexural and coupled flexural and torsional frequencies, as it is done in Section 9, Table 4. In addition, let us consider the properties of natural vibration modes calculated with constant and mode dependent stiffness parameters. In the former case modes are orthogonal, i.e.

$$\int_0^L w_i w_j dx = 0, \quad \text{if } i \neq j \tag{H16}$$

In the later case, each natural mode determined with own effective parameters can be expressed in a series of the above orthogonal modes. Since the considered modes are not orthogonal

$$\int_0^L w_i^i w_j^j \mathrm{d}x = \int_0^L \sum_{k=1}^{\infty} a_k^i w_k \sum_{l=1}^{\infty} a_l^j w_l \mathrm{d}x = \sum_{k=1}^{\infty} a_k^i a_k^j \int_0^L w_k^2 \mathrm{d}x \neq 0. \tag{H17}$$

References

[1] Mikkelsen B. Emma Maersk – The World's Largest. The Scandinavian Shipping Gazette; 2006.
[2] Bishop RED, Price WG. Hydroelasticity of Ships. Cambridge University Press; 1979.
[3] Senjanović I, Malenica Š, Tomašević S, Rudan S. Methodology of ship hydroelasticity investigation. Brodogradnja 2007; 58(2):133–45.
[4] S. Tomašević, Hydroelastic model of dynamic response of container ships in waves. Ph.D. Thesis, FSB, Zagreb, 2007 (in Croatian).
[5] Malenica Š, Senjanović I, Tomašević S, Stumpf E. Some aspects of hydroelastic issues in the design of ultra large container ships. In: The 22nd IWWWFB. Croatia: Plitvice Lakes; 2007.
[6] Remy F, Molin B, Ledoux A. Experimental and Numerical Study of the Wave Response of a Flexible Barge. Wuxi, China: Hydroelasticity in Marine Technology; 2006. pp. 255–264.
[7] Senjanović I, Malenica Š, Tomašević S. Investigation of ship hydroelasticity. Ocean Engineering 2008;35:523–35.
[8] Kawai T. The application of finite element methods to ship structures. Computers & Structures 1973;3:1175–94.
[9] Senjanović I, Grubušić R. Coupled horizontal and torsional vibration of a ship hull with large hatch openings. Computers & Structures 1991;41(2):213–26.
[10] Wu JS, Ho CS. Analysis of wave induced horizontal and torsion coupled vibrations of ship hull. Journal of Ship Research 1987;31(4):235–52.
[11] Pedersen PT. Torsional response of container ships. Journal of Ship Research 1985;29:194–205.
[12] Vlasov VZ. Thin-Walled Elastic Beams. Jerusalem: Israel Program for Scientific Translation; 1961.
[13] Haslum K, Tonnessen A. An analysis of torsion in ship hull. European Shipbuilding 1972;5/6:67–89.
[14] Senjanović I, Fan Y. A higher-order theory of thin-walled girders with application to ship structures. Computers & Structures 1992;43(1):31–52.
[15] Senjanović I, Fan Y. A higher-order flexural beam theory. Computers & Structures 1989;32(5):973–86.
[16] Senjanović I, Fan Y. A higher-order torsional beam theory. Engineering Modelling 1997;32(1–4):25–40.
[17] R. Pavazza, Bending and torsion of thin-walled beams of open section on elastic foundation. Ph.D. Thesis. University of Zagreb, 1991 (in Croatian).
[18] Pavazza R. Torsion of thin-walled beams of open cross-sections with influence of shear. International Journal of Mechanical Sciences 2005;47:1099–122.
[19] Timoshenko S, Young DH. Vibrations Problems in Engineering. D. Van Nostrand; 1955.
[20] Senjanović I. Ship Vibrations. Part 2, Textbook. Zagreb: University of Zagreb; 1990 [in Croatian].
[21] Bathe KJ. Finite Element Procedures. Englewood Cliffs, NJ: Prentice-Hall; 1996.
[22] Senjanović I. Harmonic acceleration method for dynamic structural analysis. Computers & Structures 1984;18(1):71–80.
[23] Lozina Ž. A comparison of harmonic acceleration method with the other commonly used methods for calculation of dynamic transient response. Computers & Structures 1988;29(2):227–40.
[24] Fan Y, Senjanović I. STIFF, User's Manual. Zagreb: Faculty of Mechanical Engineering and Naval Architecture; 1990.
[25] Senjanović I, Fan Y. A finite element formulation of initial ship cross-section properties. Brodogradnja 1993;41(1):27–36.
[26] Senjanović I, Ćatipović I, Tomašević S. Coupled horizontal and torsional vibrations of a flexible barge. Engineering Structures 2008;30:93–109.
[27] Senjanović I, Ćatipović I, Tomašević S. Coupled horizontal and torsional vibrations of ship-like girders. Thin-Walled Structures 2007;45:1002–21.
[28] Kilroy K. Quick Reference Guide. MSC/NASTRAN, Version 70. The MacNeal-Schwendler Corporation; 1997.
[29] Cheung YK. Finite Strip Method in Structural Analysis. Pergamon Press; 1976.
[30] Senjanović I, Fan Y. Pontoon torsional strength analysis related to ships with large deck openings. Journal of Ship Research 1991;35(4):339–51.
[31] Senjanović I, Tomašević S, Rudan S, Senjanović T. Role of transverse bulkheads in hull stiffness of large container ships. Engineering Structures 2008;30:2492–509.
[32] Szilard R. Theories and Applications of Plate Analysis. New York: John Wiley & Sons; 2004.
[33] Cowper GR. On the accuracy of Timoshenko's beam theory. Journal of Engineering Mechanics 1968;94:1447–53. American Society of Civil Engineers.
[34] Stephen NG. Considerations on second order beam theory. International Journal of Solids and Structures 1981;17:325–33.
[35] Senjanović I, Fan Y. Investigation of effective bending and shear stiffness of thin-walled girders related to ship hull vibration analysis. Journal of Ship Research 1989;33(4):298–309.
[36] Senjanović I, Fan Y. The bending and shear coefficients of thin-walled girders. Thin-Walled Structures 1990;10:31–57.
[37] Senjanović I, Fan Y. On torsional and warping stiffness of thin-walled girders. Thin-Walled Structures 1991;11:233–76.
[38] Jensen JJ. On the shear coefficient in Timoshenko's beam theory. Journal of Sound and Vibration 1983;87(4):621–35.

Ivo Senjanović, D.Sc. Professor of Naval Architecture at the Faculty of Mechanical Engineering and Naval Architecture, University of Zagreb. Teaching several courses on strength and vibration of ship and offshore structures, submarines etc. Investigation fields are ship stability, launching, numerical methods, numerical simulations, non-linear dynamics, ship strength and vibration, shell theory and design of pressure vessels. Published books on shell theory, ship vibrations and finite element method, and ca. 200 scientific and professional papers. E-mail: ivo.senjanovic@fsb.hr; http://mahazu.hazu.hr/Akademici/ISenjanovic.html.

Stipe Tomašević, Ph.D. Lecturer at the Faculty of Mechanical Engineering and Naval Architecture, University of Zagreb. Support in education on the finite element method and software application. Investigation of ship strength, vibration, fatigue and hydroelasticity. E-mail: stipe.tomasevic@fsb.hr.

Nikola Vladimir, Dipl. Ing., Ph.D. student at the Faculty of Mechanical Engineering and Naval Architecture, University of Zagreb. E-mail: nikola.vladimir@fsb.hr